

Optimal Adaptive Waveform Design for Cognitive MIMO Radar

Wasim Huleihel, Joseph Tabrikian, *Senior Member, IEEE*, and Reuven Shavit, *Senior Member, IEEE*

Abstract—This paper addresses the problem of adaptive waveform design for estimation of parameters of linear systems. This problem arises in several applications such as radar, sonar, or tomography. In the proposed technique, the transmit/input signal waveform is optimally determined at each step based on the observations in the previous steps. The waveform is determined to minimize the Bayesian Cramér-Rao bound (BCRB) or the Reuven-Messer bound (RMB) for estimation of the unknown system parameters at each step. The algorithms are tested for spatial transmit waveform design in multiple-input multiple-output radar target angle estimation at very low signal-to-noise ratio. The proposed techniques allow to automatically focusing the transmit beam toward the target direction. The simulations show that the proposed adaptive waveform design methods achieve significantly higher rate of performance improvement as a function of the pulse index, compared to other signal transmission methods, in terms of estimation accuracy.

Index Terms—Adaptive waveform design, Bayesian Cramér-Rao bound (BCRB), cognitive radar (CR), Reuven-Messer bound (RMB), waveform optimization.

I. INTRODUCTION

WAVEFORM optimization for system parameter estimation is an emerging topic in signal processing with applications in many areas, such as, radar, sonar, or tomography. The basic idea is to optimize a criterion such as, statistical bounds, probability of error, output signal-to-noise ratio (SNR), and information theoretic measures, with respect to (w.r.t.) the transmit waveform, in order to achieve better estimation or detection performance.

Multiple-input multiple-output (MIMO) radar is an emerging technology that attracts the attention of researchers and practitioners alike [1]–[5]. Unlike a standard phased-array radar, which transmits scaled versions of a single waveform, a MIMO radar system can transmit via its antennas multiple probing signals that may be different from each other. This waveform diversity offered by MIMO radar enables superior capabilities compared with a standard phased-array radar. For example, MIMO radar with colocated transmit and receive antennas has

been shown to offer higher resolution and sensitivity, better parameter identifiability and direct applicability of adaptive array techniques [4]. MIMO radar allows flexibility in the design of the transmit waveform, and hence opens a doorway for works in this field.

Waveform design for MIMO radar has been intensively investigated in the recent years (see e.g. [6]–[19]). Waveform optimization for MIMO radar target localization using the Cramér-Rao bound (CRB), was considered in [6] for single target case. This approach was generalized for the case of multiple targets in [7]. In [8], [11], waveform design based on mutual information and minimum mean-square-error (MMSE) was considered and it was shown that by using optimized waveforms one can achieve better detection performance and greater mutual information. In [13], signal design for MIMO radar based on transmit beampattern was considered and it was shown that in order to significantly improve the estimation performance, the transmit beampattern should be focused at the target direction. In [9] it was shown that maximizing the mutual information (MI) between the target impulse response and the observations may enable the radar system a better capability in characterizing a target in noisy environment. In [10] some interesting extensions including MI-based waveform design in the presence of multiple targets were considered. In [11] space-time code optimization for MIMO radar based on MI was considered. Other waveform design methods based on information theoretic measures can be found in [8], [14], [18].

The idea of cognitive radar (CR) was proposed in [20] and investigated in several works (see e.g. [21]–[24]). A cognitive radar system adaptively interrogates the propagation channel using the available information from previous observations, external databases, and task priorities. This implies that the transmit waveforms can be sequentially adapted based on the information collected in the previous observations about the environment and the targets. In [22] two different waveform design techniques based on sequential hypothesis testing for active sensors operating in a target recognition application were derived. In [23] an algorithm for optimal waveform design for CR based on maximizing the output SNR and the mutual information between the target ensemble and observations, was derived.

Adaptive design and processing of waveforms has been applied for target tracking applications, for example in [25]–[32]. In [25] an adaptive polarized waveform design for target tracking based on sequential Bayesian inference was considered. In [26] adaptive methods for target tracking and active sensing have been studied in a several contexts. In [27] a waveform design algorithm based on MI for MIMO radar target tracking was derived using wideband orthogonal frequency division multiplexing (OFDM) signaling scheme. In [28], [29]

Manuscript received November 02, 2012; revised March 11, 2013 and May 26, 2013; accepted May 28, 2013. Date of publication June 17, 2013; date of current version September 11, 2013. The associate editor coordinating the review of this manuscript and approving it for publication was Prof. Maria Sabrina Greco. This work was supported in part by The Israel Science Foundation (Grant 1392/11).

The authors are with the Department of Electrical and Computer Engineering, Ben-Gurion University of the Negev Beer-Sheva 84105, Israel (e-mail: wasim8@gmail.com; joseph@ee.bgu.ac.il; rshavit@ee.bgu.ac.il).

Color versions of one or more of the figures in this paper are available online at <http://ieeexplore.ieee.org>.

Digital Object Identifier 10.1109/TSP.2013.2269045

an optimal waveform design technique based on minimum mean-square tracking error and minimum validation gate, for single target in white Gaussian noise using conventional Kalman filter tracker was derived, and generalized to trackers looking one and two steps ahead in [32]. In [30], [31] optimal waveform design based on minimizing the mean-square tracking error was proposed for linear Gaussian state model and a nonlinear Gaussian measurement model.

In this paper, we propose a new technique for adaptive transmit waveform design for target estimation in MIMO radar. Instead of transmission of a pulse train with predefined waveform, each waveform in the pulse train is adaptively determined based on the previously received data, often referred as memory or history. The considered observation model is general and represents any linear system with unknown parameters and additive Gaussian noise, which is useful in many applications such as radar, sonar, or tomography. The Bayesian Cramér Rao bound (BCRB) [33] or the Reuven-Messer bound (RMB) [34] are used as criteria for waveform optimization. We propose an approach for transmit waveform design, which adaptively minimizes the BCRB and the RMB on the system parameter estimation based on previous received data. The main advantage of the proposed method is that it is capable to automatically focus on the target after a few trials/pulses, at very low SNRs.

We adopt a Bayesian approach, since in general, non-Bayesian bounds may depend on the unknown parameters to be estimated and therefore, optimal waveforms with these criteria may also depend on the unknown parameters (see e.g. [6]). Furthermore, in many problems, such as tracking, some prior statistical information on the parameters may be available, and the use of Bayesian bounds in such problems is natural. The BCRB criterion provides a simpler procedure for waveform design compared to the RMB criterion. However, since the BCRB considers only small errors, an optimal waveform under this criterion may result in waveforms which lead to high sidelobes in the posterior function. Conversely, since the RMB takes into account the contribution of large errors due to high sidelobes, its use as a criterion for waveform design allows controlling the sidelobes based on the posterior distribution, and therefore, reduces the threshold SNR. It should be noticed that controlling the sidelobes does not necessarily mean lower sidelobes in the beampattern, since the criterion may allow high sidelobes towards directions with low probability of existence of a target.

The rest of this paper is organized as follows. In Section II, the system model is described and the problem is formulated. In Sections III and IV, adaptive transmit waveform design techniques are derived using the optimization criteria BCRB and RMB, respectively. In Section V, the performance of the proposed techniques are evaluated and compared to other known waveform design methods for the problem of target localization by MIMO radar. Finally, our conclusions appear in Section VI.

II. MODEL AND PROBLEM FORMULATION

Consider the following general data model which is useful in many applications such as radar, sonar, or tomography

$$\mathbf{x}_{k,l} = \mathbf{H}_k(\boldsymbol{\theta})\mathbf{s}_{k,l} + \mathbf{n}_{k,l}, \quad l = 1, \dots, L, \quad k = 1, 2, \dots \quad (1)$$

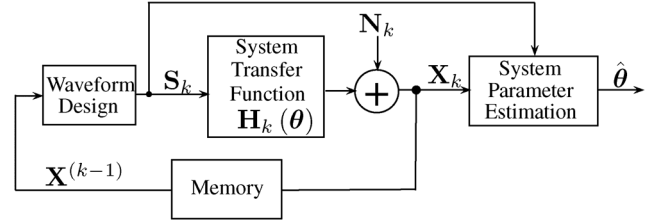


Fig. 1. Cognitive scheme for linear system with additive noise.

where $\mathbf{x}_{k,l} \in \mathbb{C}^{N_R}$, $\mathbf{s}_{k,l} \in \mathbb{C}^{N_T}$, and $\mathbf{n}_{k,l} \in \mathbb{C}^{N_R}$ denote the l th snapshot of the data, the transmit/input signal, and the noise vectors, respectively, at the k th step/pulse index, and L is the number of snapshots at each step. The matrix $\mathbf{H}_k(\boldsymbol{\theta}) \in \mathbb{C}^{N_R \times N_T}$ stands for the system transfer function, which depends on the unknown random vector $\boldsymbol{\theta} \in \mathbb{R}^Q$ with *a-priori* probability density function (pdf) $f_{\boldsymbol{\theta}}(\cdot)$. We assume that $\mathbf{H}_k(\cdot)$ is a known function. In radar systems for example, the vector $\boldsymbol{\theta}$ may consist of targets directions, ranges, complex amplitudes, and environmental or array parameters.

Equation (1) can be rewritten in matrix form as

$$\mathbf{X}_k = \mathbf{H}_k(\boldsymbol{\theta})\mathbf{S}_k + \mathbf{N}_k, \quad k = 1, 2, \dots \quad (2)$$

where $\mathbf{X}_k = [\mathbf{x}_{k,1}, \dots, \mathbf{x}_{k,L}]$, $\mathbf{S}_k = [\mathbf{s}_{k,1}, \dots, \mathbf{s}_{k,L}]$, and $\mathbf{N}_k = [\mathbf{n}_{k,1}, \dots, \mathbf{n}_{k,L}]$. We assume that the columns of \mathbf{N}_k are independent and identically distributed (i.i.d.) complex circularly symmetric Gaussian random vectors with zero mean and known covariance matrix \mathbf{R} .

We are interested in the design of the transmit signal matrix at the k th step, denoted by \mathbf{S}_k , given observations in previous steps (history), denoted by $\mathbf{X}^{(k-1)} = [\mathbf{X}_1, \dots, \mathbf{X}_{k-1}]$. Fig. 1 describes the considered cognitive scheme. The transmit signal energy is constrained, i.e. $\text{tr}(\frac{1}{L}\mathbf{S}_k\mathbf{S}_k^H) = P$, where P denotes the total transmit energy at each snapshot, and $\text{tr}(\cdot)$ denotes the matrix trace operator. This problem can be formulated as follows

$$\begin{aligned} & \underset{\mathbf{S}_k}{\text{optimize}} \quad C(\mathbf{S}_k, \mathbf{X}^{(k-1)}) \\ & \text{s.t.} \quad \text{tr}\left(\frac{1}{L}\mathbf{S}_k\mathbf{S}_k^H\right) = P \end{aligned} \quad (3)$$

where $C(\cdot, \cdot)$ denotes the objective or utility function, defined on the real numbers. In this paper, two utility functions (optimization criteria) are considered; the BCRB and the RMB, on the estimation performance of $\boldsymbol{\theta}$ from $\mathbf{X}^{(k)}$.

In practice, the noise covariance matrix, \mathbf{R} , may be unknown. In such a case, a possible ad-hoc method is to estimate the noise covariance matrix based on the history, and update it from pulse to pulse. In the following, we assume that \mathbf{R} is perfectly known.

III. ADAPTIVE WAVEFORM OPTIMIZATION—BCRB

In this section, we propose a new method for adaptive transmit waveform design for the general model presented in the previous section. At each step (pulse index), the algorithm determines the transmit waveform in order to optimize the estimation performance in terms of the BCRB. In the following, we first present the conditional BCRB at the k th step, given previous observations $\mathbf{X}^{(k-1)}$. Then, we determine the transmit waveform design, which minimizes the conditional BCRB in the scalar case, i.e. single unknown parameter θ to be estimated

($Q = 1$). Finally, we generalize the analysis to the case of unknown random vector $\boldsymbol{\theta}$.

A. Optimization Criterion

As mentioned above, we are interested in the design of the transmit signal matrix at the k th step, \mathbf{S}_k , given history observations $\mathbf{X}^{(k-1)}$, such that at each step we aim to optimize the estimation performance of $\boldsymbol{\theta}$ in terms of MSE. Accordingly, we wish to minimize the following MSE matrix w.r.t. \mathbf{S}_k

$$\mathbf{\Pi}_k \triangleq \mathbb{E} \left[(\hat{\boldsymbol{\theta}}_k - \boldsymbol{\theta})(\hat{\boldsymbol{\theta}}_k - \boldsymbol{\theta})^T \right] \quad (4)$$

where $\hat{\boldsymbol{\theta}}_k$ is the MMSE estimator of $\boldsymbol{\theta}$ at the k th step. Using the law of total expectation, (4) can be rewritten as

$$\mathbf{\Pi}_k = \mathbb{E} \left\{ \mathbb{E} \left[(\hat{\boldsymbol{\theta}}_k - \boldsymbol{\theta})(\hat{\boldsymbol{\theta}}_k - \boldsymbol{\theta})^T | \mathbf{X}^{(k-1)} \right] \right\}. \quad (5)$$

The outer expectation of (5) is performed w.r.t. the pdf of $\mathbf{X}^{(k-1)}$, which is independent of \mathbf{S}_k . Therefore, minimization of (5) w.r.t. \mathbf{S}_k can be performed by minimizing the inner term in the outer expectation of (5) independently for each $\mathbf{X}^{(k-1)}$. Accordingly, minimizing (4) is equivalent to minimizing the conditional MMSE matrix, $\mathbf{\Sigma}_k$, defined as

$$\mathbf{\Sigma}_k = \mathbb{E} \left[(\hat{\boldsymbol{\theta}}_k - \boldsymbol{\theta})(\hat{\boldsymbol{\theta}}_k - \boldsymbol{\theta})^T | \mathbf{X}^{(k-1)} \right]. \quad (6)$$

Since it is difficult to obtain an analytical expression for $\mathbf{\Sigma}_k$, we will consider minimization of its lower bound.

The conditional BCRB is a lower bound on the conditional MSE matrix, and provides a ‘‘global bound’’ that does not depend on the actual value of the unknown parameter $\boldsymbol{\theta}$. Unlike the classic BCRB [33], the conditional BCRB [35] utilizes the information contained in the available history measurements. The conditional covariance matrix $\mathbf{\Sigma}_k$, satisfies [35]

$$\mathbf{\Sigma}_k \succeq \mathbf{J}_k^{-1} \triangleq \mathbf{C}_k^{(\text{BCRB})} \quad (7)$$

where \mathbf{J}_k and $\mathbf{C}_k^{(\text{BCRB})}$ denote the conditional Fisher information matrix (FIM), and the conditional BCRB at step k , respectively, and $\succeq \mathbf{0}$ denotes a positive semidefinite sign. Let $f_{\mathbf{X}_k | \mathbf{X}^{(k-1)}, \boldsymbol{\theta}}$ denote the conditional pdf of \mathbf{X}_k given $(\mathbf{X}^{(k-1)}, \boldsymbol{\theta})$ with $f_{\mathbf{X}_1 | \mathbf{X}^{(0)}, \boldsymbol{\theta}} \triangleq f_{\mathbf{X}_1 | \boldsymbol{\theta}}$, and $f_{\boldsymbol{\theta} | \mathbf{X}^{(k-1)}}$ denote the conditional pdf of $\boldsymbol{\theta}$ given $\mathbf{X}^{(k-1)}$ with $f_{\boldsymbol{\theta} | \mathbf{X}^{(0)}} \triangleq f_{\boldsymbol{\theta}}$. The (i, j) element of \mathbf{J}_k , is given by

$$\begin{aligned} [\mathbf{J}_k]_{i,j} &\triangleq -\mathbb{E} \left(\frac{\partial^2 \log f_{\mathbf{X}_k, \boldsymbol{\theta} | \mathbf{X}^{(k-1)}}}{\partial \theta_i \partial \theta_j} \Big| \mathbf{X}^{(k-1)} \right) \\ &= [\mathbf{J}_{P_{k-1}}]_{i,j} + [\Delta \mathbf{J}_{D_k}]_{i,j} \end{aligned} \quad (8)$$

where the last equality stems from Bayes theorem, and $\Delta \mathbf{J}_{D_k}$ is the data incremental Bayesian Fisher information (IBFI), defined as

$$[\Delta \mathbf{J}_{D_k}]_{i,j} = -\mathbb{E} \left(\frac{\partial^2 \log f_{\mathbf{X}_k | \mathbf{X}^{(k-1)}, \boldsymbol{\theta}}}{\partial \theta_i \partial \theta_j} \Big| \mathbf{X}^{(k-1)} \right), \quad (9)$$

and $\mathbf{J}_{P_{k-1}}$ is the FIM due to the statistical information from history, defined as

$$[\mathbf{J}_{P_{k-1}}]_{i,j} = -\mathbb{E} \left(\frac{\partial^2 \log f_{\boldsymbol{\theta} | \mathbf{X}^{(k-1)}}}{\partial \theta_i \partial \theta_j} \Big| \mathbf{X}^{(k-1)} \right). \quad (10)$$

Note that the expectations in (9) and (10) are performed w.r.t. the conditional pdf of $(\mathbf{X}_k, \boldsymbol{\theta} | \mathbf{X}^{(k-1)})$, and the conditional pdf of $(\boldsymbol{\theta} | \mathbf{X}^{(k-1)})$, respectively. For simplicity of notations, we omit the dependency of $\Delta \mathbf{J}_{D_k}$ and $\mathbf{J}_{P_{k-1}}$ on $\mathbf{X}^{(k-1)}$.

For scalar parameter case considered in the next subsection, $C(\mathbf{S}_k, \mathbf{X}^{(k-1)})$ will be given by the BCRB, while for vector parameter case, considered in Section III-C, we will choose $C(\mathbf{S}_k, \mathbf{X}^{(k-1)}) = \text{tr}(\mathbf{W} \mathbf{C}_k^{(\text{BCRB})})$, where \mathbf{W} is a weighting matrix.

B. Scalar Parameter Case

In this subsection, we derive an adaptive transmit waveform design in the case of scalar unknown parameter θ to be estimated ($Q = 1$). By using the expression for the Fisher information in case of deterministic signal in Gaussian noise [36], and applying the law of total expectation, ΔJ_{D_k} can be written as [37]

$$\begin{aligned} \Delta J_{D_k} &= -\mathbb{E} \left(\frac{\partial^2 \log f_{\mathbf{X}_k | \mathbf{X}^{(k-1)}, \theta}}{\partial \theta^2} \Big| \mathbf{X}^{(k-1)} \right) \\ &= \mathbb{E} \left[-\mathbb{E} \left(\frac{\partial^2 \log f_{\mathbf{X}_k | \mathbf{X}^{(k-1)}, \theta}}{\partial \theta^2} \Big| \mathbf{X}^{(k-1)}, \theta \right) \Big| \mathbf{X}^{(k-1)} \right] \\ &= 2LE \left[\text{tr} \left(\dot{\mathbf{H}}_k^H \mathbf{R}^{-1} \dot{\mathbf{H}}_k \mathbf{R}_{S_k} \right) \Big| \mathbf{X}^{(k-1)} \right] \end{aligned} \quad (11)$$

where the expectation in (11) is taken w.r.t. $f_{\theta | \mathbf{X}^{(k-1)}}$, $\dot{\mathbf{H}}_k \triangleq \frac{d\mathbf{H}_k(\theta)}{d\theta}$ and $\mathbf{R}_{S_k} \triangleq \frac{1}{L} \mathbf{S}_k \mathbf{S}_k^H$. For simplicity of notations, we omit the dependency of $\dot{\mathbf{H}}_k$ on θ , and of ΔJ_{D_k} on $\mathbf{X}^{(k-1)}$. Using (10) and (11), the conditional Fisher information in (8) can be expressed as

$$\mathbf{J}_k = \mathbf{J}_{P_{k-1}} + 2L \text{tr} \left[\mathbb{E} \left(\dot{\mathbf{H}}_k^H \mathbf{R}^{-1} \dot{\mathbf{H}}_k | \mathbf{X}^{(k-1)} \right) \mathbf{R}_{S_k} \right]. \quad (12)$$

We aim to find the transmit signal matrix, \mathbf{S}_k , which minimizes the BCRB at the k th step, C_k . Based on (12), the BCRB depends on the transmit waveform only through \mathbf{R}_{S_k} , and therefore, the optimization will be performed w.r.t. the transmit signal auto-correlation matrix \mathbf{R}_{S_k} . By using (7) and noticing that $\mathbf{J}_{P_{k-1}}$ in (12) is independent of \mathbf{R}_{S_k} , minimization of BCRB, $C_k^{(\text{BCRB})}$, under the total energy constraint can be stated as

$$\begin{aligned} \bar{\mathbf{R}}_{S_k} &= \arg \max_{\mathbf{R}_{S_k}} \text{tr} \left[\mathbb{E} \left(\dot{\mathbf{H}}_k^H \mathbf{R}^{-1} \dot{\mathbf{H}}_k | \mathbf{X}^{(k-1)} \right) \mathbf{R}_{S_k} \right] \\ &\text{s.t. } \text{tr}(\mathbf{R}_{S_k}) = P, \quad \mathbf{R}_{S_k} \succeq \mathbf{0}. \end{aligned} \quad (13)$$

Let

$$\mathbf{\Gamma}_k \left(\mathbf{X}^{(k-1)} \right) \triangleq \mathbb{E} \left(\dot{\mathbf{H}}_k^H \mathbf{R}^{-1} \dot{\mathbf{H}}_k | \mathbf{X}^{(k-1)} \right). \quad (14)$$

Then, by using the singular value decomposition (SVD) of \mathbf{R}_{S_k} and $\bar{\mathbf{R}}_{S_k} : \mathbf{R}_{S_k} = \mathbf{U}_k \mathbf{\Lambda}_k \mathbf{U}_k^H$ and $\bar{\mathbf{R}}_{S_k} = \bar{\mathbf{U}}_k \bar{\mathbf{\Lambda}}_k \bar{\mathbf{U}}_k^H$, the maximization problem in (13) becomes

$$\begin{aligned} (\bar{\mathbf{U}}_k, \bar{\mathbf{\Lambda}}_k) &= \arg \max_{\mathbf{U}_k, \mathbf{\Lambda}_k} \text{tr} \left[\mathbf{U}_k^H \mathbf{\Gamma}_k \left(\mathbf{X}^{(k-1)} \right) \mathbf{U}_k \mathbf{\Lambda}_k \right] \\ &\text{s.t. } \text{tr}(\mathbf{\Lambda}_k) = P, \quad \mathbf{\Lambda}_k \succeq \mathbf{0}, \\ &\text{and } \mathbf{U}_k \text{ is unitary.} \end{aligned} \quad (15)$$

Denoting $\mathbf{\Lambda}_k = \text{diag}(\lambda_{1,k}, \dots, \lambda_{N_T,k})$, and $\mathbf{U}_k = [\mathbf{u}_{1,k}, \dots, \mathbf{u}_{N_T,k}]$, where $\text{diag}(\cdot)$ denotes the diagonal operator, the maximization problem in (15) can be rewritten as

$$\begin{aligned} (\bar{\mathbf{U}}_k, \bar{\mathbf{\Lambda}}_k) = & \arg \max_{\mathbf{U}_k, \mathbf{\Lambda}_k} \sum_{i=1}^{N_T} \gamma_k(\mathbf{u}_{i,k}) \lambda_{i,k} \\ \text{s.t.} \quad & \sum_{i=1}^{N_T} \lambda_{i,k} = P, \lambda_{i,k} \geq 0, i = 1, \dots, N_T \end{aligned} \quad (16)$$

where $\gamma_k(\mathbf{u}_{i,k}) = \mathbf{u}_{i,k}^H \mathbf{\Gamma}_k(\mathbf{X}^{(k-1)}) \mathbf{u}_{i,k}$. Since $\{\lambda_{i,k}\}_{i=1}^{N_T}$ are non-negative, then the objective function in (16) is maximized by assigning all the available power on the subspace with maximum $\gamma_k(\mathbf{u}_{i,k})$, and zero power on the complement subspace. The vector $\mathbf{u}_{i,k}$ which maximizes $\gamma_k(\mathbf{u}_{i,k})$ is given by the eigenvector corresponding to the maximum eigenvalue of $\mathbf{\Gamma}_k(\mathbf{X}^{(k-1)})$. Denoting this eigenvector by $\bar{\mathbf{u}}_k$, the solution of the maximization problem in (16) is

$$\begin{aligned} \bar{\mathbf{\Lambda}}_k &= \text{diag}(P, 0, \dots, 0) \\ \bar{\mathbf{U}}_k &= [\bar{\mathbf{u}}_k, \mathbf{V}_k] \end{aligned} \quad (17)$$

where \mathbf{V}_k denotes a matrix of size $N_T \times (N_T - 1)$, whose columns are orthonormal and perpendicular to $\bar{\mathbf{u}}_k$. Based on (17), the transmit signal auto-correlation matrix is given by

$$\bar{\mathbf{R}}_{\mathbf{S}_k} = P \cdot \bar{\mathbf{u}}_k \bar{\mathbf{u}}_k^H. \quad (18)$$

C. Vector Parameter Case

We now derive the optimal transmit waveform in the case of unknown random vector $\boldsymbol{\theta}$. In Appendix A, it is shown that the matrix $\Delta \mathbf{J}_{D_k}$ in (9) for the model described in Section II, is given by

$$\Delta \mathbf{J}_{D_k} = 2L \text{Re} \left\{ \mathbf{Q}_I \left[\tilde{\mathbf{\Gamma}}_k(\mathbf{X}^{(k-1)}) \odot (\mathbf{1}_{Q \times Q} \otimes \mathbf{R}_{\mathbf{S}_k}^T) \right] \mathbf{Q}_I^T \right\}, \quad (19)$$

in which

$$\tilde{\mathbf{\Gamma}}_k(\mathbf{X}^{(k-1)}) \triangleq \text{E} \left(\hat{\mathbf{H}}_k^H \mathbf{R}^{-1} \hat{\mathbf{H}}_k | \mathbf{X}^{(k-1)} \right) \quad (20)$$

where $\text{Re}(\cdot)$, \odot , and \otimes are the real part operator, Hadamard, and Kronecker products, respectively. The matrix $\mathbf{1}_{Q \times Q}$ is a $Q \times Q$ matrix whose elements are equal to one, $\hat{\mathbf{H}}_k$ is an $N_R \times N_T Q$ matrix, defined in (46), and \mathbf{Q}_I is a $Q \times N_T Q$ matrix, defined in (51).

The matrix $\mathbf{J}_{P_{k-1}}$ defined in (10), is independent of \mathbf{S}_k , and by using (7), (8), and (19), we conclude that the BCRB, $\mathbf{C}_k^{(\text{BCRB})}$, is a function of the transmit waveform only through the signal auto-correlation matrix. Accordingly, we aim to find the transmit signal auto-correlation matrix, which ‘‘optimizes’’ the BCRB at the k th step, $\mathbf{C}_k^{(\text{BCRB})}$. Since the BCRB in this case is a matrix, various optimization criteria can be chosen, e.g. minimizing the trace, the determinant, or the largest eigenvalue of the BCRB, w.r.t. the transmit auto-correlation matrix. Note that according to (19), the data FIM at step k is a linear function of the auto-correlation matrix $\mathbf{R}_{\mathbf{S}_k}$. Therefore, each one of the criteria mentioned above, under the constraints $\mathbf{R}_{\mathbf{S}_k} \succeq \mathbf{0}$, and $\text{tr}(\mathbf{R}_{\mathbf{S}_k}) = P$, leads to a convex optimization problem [38, Ch. 3] that can be solved efficiently (in polynomial time)

TABLE I
ADAPTIVE WAVEFORM DESIGN ALGORITHM BASED ON BCRB

Initialization: Set $k = 1$, $f_{\boldsymbol{\theta} \mathbf{x}_0} = f_{\boldsymbol{\theta}}$.
1. Using the component-wise updating MH sampler and (24), produce N_s samples from the posterior pdf $f_{\boldsymbol{\theta} \mathbf{X}^{(k-1)}}$.
2. Compute $\tilde{\mathbf{\Gamma}}_k(\mathbf{X}^{(k-1)})$ given in (20).
3. Construct $\Delta \mathbf{J}_{D_k}$ and compute $\mathbf{J}_{P_{k-1}}$ given in (19) and (23), respectively, where the expectations are calculated via MC integration.
4. Construct $\bar{\mathbf{R}}_{\mathbf{S}_k}$ according to (22).
5. Construct a signal waveform \mathbf{S}_k with auto-correlation matrix $\bar{\mathbf{R}}_{\mathbf{S}_k}$ and obtain measurement \mathbf{X}_k .
6. Set $k \leftarrow k + 1$ and go to step 1.

using interior point methods [39]. In the following, we consider the trace optimization criterion, although other criteria can be readily considered. Under the considerations described above, the optimization problem can be stated as

$$\begin{aligned} \bar{\mathbf{R}}_{\mathbf{S}_k} &= \arg \min_{\mathbf{R}_{\mathbf{S}_k}} \text{tr} \left(\mathbf{W} \mathbf{C}_k^{(\text{BCRB})} \right) \\ \text{s.t.} \quad & \text{tr}(\mathbf{R}_{\mathbf{S}_k}) = P, \quad \mathbf{R}_{\mathbf{S}_k} \succeq \mathbf{0} \end{aligned} \quad (21)$$

where $\mathbf{W} = \text{diag}(w_1, \dots, w_Q)$ is a positive-definite weighting matrix, which can be used to weight the MSE bound of each parameter in $\boldsymbol{\theta}$, or perhaps to balance the units used for different parameters.

The waveform optimization problem based on this criterion can be cast as a semidefinite programming (SDP) [40] using straight-forward algebraic manipulations. It was shown in [7], [40] that the minimization problem in (21) can be cast as the following SDP problem

$$\begin{aligned} \bar{\mathbf{R}}_{\mathbf{S}_k} &= \arg \min_{\mathbf{R}_{\mathbf{S}_k}} \min_{\{t_l\}_{l=1}^Q} \sum_{l=1}^Q w_l t_l \\ \text{s.t.} \quad & \begin{bmatrix} \Delta \mathbf{J}_{D_k} + \mathbf{J}_{P_{k-1}} & \mathbf{e}_i \\ \mathbf{e}_i^T & t_i \end{bmatrix} \succeq \mathbf{0}, \quad i = 1, \dots, Q \\ & \text{tr}(\mathbf{R}_{\mathbf{S}_k}) = P, \quad \mathbf{R}_{\mathbf{S}_k} \succeq \mathbf{0} \end{aligned} \quad (22)$$

where $\{t_l\}_{l=1}^Q$ are auxiliary variables, the matrix $\Delta \mathbf{J}_{D,k}$ is given in (19), which is a linear function of $\mathbf{R}_{\mathbf{S}_k}$, and \mathbf{e}_i denotes the i th column of the identity matrix. Finally, note that the constraints in the above SDP are either linear matrix inequalities or linear equalities in the elements of the transmit auto-correlation matrix $\mathbf{R}_{\mathbf{S}_k}$.

According to (22), in order to find $\bar{\mathbf{R}}_{\mathbf{S}_k}$, the matrix $\mathbf{J}_{P_{k-1}}$ is required. In Appendix B, it is shown that the matrix $\mathbf{J}_{P_{k-1}}$ is given by

$$\begin{aligned} \mathbf{J}_{P_{k-1}} &= \mathbf{J}_{I_{k-1}} + \mathbf{J}_{N_{k-1}} \\ &+ 2L \sum_{m=1}^{k-1} \text{Re} \left\{ \mathbf{Q}_I \left[\tilde{\mathbf{\Gamma}}_m(\mathbf{X}^{(k-1)}) \odot (\mathbf{1}_{Q \times Q} \otimes \mathbf{R}_{\mathbf{S}_m}^T) \right] \mathbf{Q}_I^T \right\} \end{aligned} \quad (23)$$

where the matrices $\mathbf{J}_{I_{k-1}}$ and $\mathbf{J}_{N_{k-1}}$ are defined in (56) and (57), respectively.

D. Recursive Computation of Posterior PDF

The construction of (19) and (23), involves calculation of some conditional expectations w.r.t. the posterior pdf $f_{\boldsymbol{\theta}|\mathbf{X}^{(k-1)}}$ via $\tilde{\mathbf{\Gamma}}_k$, $\mathbf{J}_{I_{k-1}}$, and $\mathbf{J}_{N_{k-1}}$ defined in (20), (56), and (57), respectively. In order to compute these matrices, one needs to calculate

the posterior pdf $f_{\boldsymbol{\theta}|\mathbf{X}^{(k-1)}}$, which can be recursively updated. In this subsection, an efficient method for recursive computation of the posterior pdf is presented.

Proposition 1 (Iterative Calculation of $f_{\boldsymbol{\theta}|\mathbf{X}^{(k-1)}}$): Let $F_0(\boldsymbol{\theta}) \triangleq f_{\boldsymbol{\theta}}$ and $f_{\mathbf{X}_1|\mathbf{X}^{(0)},\boldsymbol{\theta}} = f_{\mathbf{X}_1|\boldsymbol{\theta}}$. Then, the posterior pdf $f_{\boldsymbol{\theta}|\mathbf{X}^{(k-1)}}$ is given by

$$f_{\boldsymbol{\theta}|\mathbf{X}^{(k-1)}} = \frac{F_{k-1}(\boldsymbol{\theta})}{f_{\mathbf{X}^{(k-1)}}} \quad k = 2, 3, \dots \quad (24)$$

where $F_{k-1}(\boldsymbol{\theta})$ can be recursively computed by

$$F_{k-1}(\boldsymbol{\theta}) = F_{k-2}(\boldsymbol{\theta}) \cdot f_{\mathbf{X}_{k-1}|\mathbf{X}^{(k-2)},\boldsymbol{\theta}}. \quad (25)$$

Proof: Using Bayes theorem, (25) implies that

$$\begin{aligned} F_{k-1}(\boldsymbol{\theta}) &= F_0(\boldsymbol{\theta}) \prod_{m=1}^{k-1} f_{\mathbf{X}_m|\mathbf{X}^{(m-1)},\boldsymbol{\theta}} \\ &= \underbrace{f_{\mathbf{X}_1|\boldsymbol{\theta}} F_0(\boldsymbol{\theta})}_{f_{\mathbf{X}_1,\boldsymbol{\theta}}} \prod_{m=2}^{k-1} f_{\mathbf{X}_m|\mathbf{X}^{(m-1)},\boldsymbol{\theta}} \\ &= f_{\mathbf{X}_2,\mathbf{X}_1,\boldsymbol{\theta}} \prod_{m=3}^{k-1} f_{\mathbf{X}_m|\mathbf{X}^{(m-1)},\boldsymbol{\theta}} \\ &= \dots = f_{\mathbf{X}_{k-1},\dots,\mathbf{X}_1,\boldsymbol{\theta}} = f_{\mathbf{X}^{(k-1)},\boldsymbol{\theta}}. \end{aligned} \quad (26)$$

Hence, using (26) and Bayes theorem, one obtains

$$\frac{F_{k-1}(\boldsymbol{\theta})}{f_{\mathbf{X}^{(k-1)}}} = \frac{1}{f_{\mathbf{X}^{(k-1)}}} f_{\mathbf{X}^{(k-1)},\boldsymbol{\theta}} = f_{\boldsymbol{\theta}|\mathbf{X}^{(k-1)}}. \quad (27)$$

For evaluation of the recursive equation in (25), one needs to compute pdf's of the form $f_{\mathbf{X}_k|\mathbf{X}^{(k-1)},\boldsymbol{\theta}}$. In our case, it can be easily verified that $(\mathbf{X}_k|\mathbf{X}^{(k-1)},\boldsymbol{\theta}) \sim \mathcal{N}^c(\mathbf{H}_k(\boldsymbol{\theta})\mathbf{S}_k(\mathbf{X}^{(k-1)}), \mathbf{R})$. Moreover, note that the denominator in (24) is a normalization factor, independent of $\mathbf{R}_{\mathbf{S}_k}$, which only scales the objective function of the minimization problem in (21) via both $\Delta\mathbf{J}_{D_k}$ and $\mathbf{J}_{P_{k-1}}$. Hence, it has no impact on the optimal solution of (21) and can be ignored.

In addition to the computation of the posterior pdf, evaluation of (20) and (55)–(57) involves some expectations w.r.t. the posterior pdf $f_{\boldsymbol{\theta}|\mathbf{X}^{(k-1)}}$. These expectations can be computed numerically using Monte-Carlo (MC) integration, where samples of the unknown parameters $\boldsymbol{\theta}$ are obtained from $f_{\boldsymbol{\theta}|\mathbf{X}^{(k-1)}}$, using the *component-wise updating* Metropolis-Hastings (MH) sampling approach [41], [42]. In order to use the MH sampler, the so-called *proposal distribution* should be chosen. A popular choice is the Gaussian distribution with first and second order statistics which are judiciously determined. In our settings, in each pulse index the first and second order statistics of the considered Gaussian proposal distribution were chosen as an estimate of the mean and variance of the samples obtained from previous pulse indices. The number of samples N_s was heuristically determined to be proportional to the standard deviation of the samples. That is to say, at the first pulse indices, a large number of samples are taken into account for the initial uncertainty, and as the pulse index increases and the standard deviation of the samples decreases, a smaller number of samples are taken.

The proposed adaptive waveform design algorithm is summarized in Table I.

E. Computational Complexity

In this subsection, we analyze the computational complexity of the proposed waveform design technique at the k th pulse index. Following Table I, the computation complexity of the proposed algorithm is approximately equal to the summation of the following factors. As previously mentioned, we use a Gaussian proposal for the MH sampler. Accordingly, at each iteration of the MH sampler (step 1 in Table I) and for each parameter, the complexity is approximately $\mathcal{O}(N_R N_T L k + N_R^2 L k + N_R L k)$ [41] which results from matrix products and summations performed in order to construct the Gaussian proposal. Since N_s samples are taken for each one of the Q parameters, the number of operations of step 1 is of order $Q N_s \mathcal{O}(N_R N_T L k + N_R^2 L k + N_R L k)$. The complexity of constructing $\Delta\mathbf{J}_{D_k}$ and computing $\mathbf{J}_{P_{k-1}}$ given in (19) and (23), respectively, using MC integration (step 2 in Table I) is approximately $N_s \mathcal{O}(N_R N_T^2 Q^2)$ [41]. Finally, the computation complexity of constructing the optimal auto-correlation matrix, $\overline{\mathbf{R}}_{\mathbf{S}_k}$, via an SDP optimization problem (step 3 in Table I) is approximately $\mathcal{O}(\sqrt{\log N_T})$ [38]. Summing up the aforementioned factors, the number of operations due to the significant factors is of order $Q N_s \mathcal{O}(N_R N_T L k + N_R^2 L k) + N_s \mathcal{O}(N_R N_T^2 Q^2)$.

IV. ADAPTIVE WAVEFORM OPTIMIZATION—RMB

The advantage of the BCRB is its simplicity and tightness at high SNRs or number of observations. However, at low SNRs and/or number of observations, large errors can occur due to existence of dominant sidelobes in the posterior pdf. These errors which result in threshold phenomenon, are ignored by the BCRB. Accordingly, waveform design based on the BCRB may result in waveforms with high sidelobes in the posterior pdf. Large-error bounds, such as RMB and Weiss-Weinstein bound [43], take into account the contribution of large errors due to sidelobes, and may predict the threshold phenomenon. The use of large-error bounds as a criterion for waveform design is expected to control the sidelobes in the posterior pdf, and result in better performance, especially at low SNRs or small number of observations.

In this section, we derive an adaptive transmit waveform design technique such that at each step the transmit waveform is determined to optimize the estimation performance in terms of RMB. As in the previous section, we use the conditional version of the classic RMB. In the next subsection, we derive the conditional RMB at the k th step given previous observations $\mathbf{X}^{(k-1)}$. Then, the transmit waveform, which optimizes the conditional RMB, is determined.

A. Conditional RMB

We now derive a criterion based on the RMB on the estimation MSE of the unknown random vector $\boldsymbol{\theta}$. The classic RMB utilizes only the statistical information on the history observations. Since history observations, $\mathbf{X}^{(k-1)}$, are available at the k th step, we are interested in the conditional RMB given $\mathbf{X}^{(k-1)}$.

Proposition 2 (Conditional RMB): Let Ω be an observation space of points \mathbf{X}_k , and let $\Theta \subseteq \mathbb{R}^Q$ be the parameter space. The

TABLE II
TRANSMIT AUTO-CORRELATION CALCULATION BASED ON RMB

Initialization: Set $k = 1$, $f_{\theta \mathbf{x}_0} = f_{\theta}$.
1. Using the component-wise updating MH sampler, produce N_s samples from the posterior pdf $f_{\theta \mathbf{x}^{(k-1)}}$.
2. Construct $\mathbf{R}_{\mathbf{S}_k}^{(n)}$ using the iterative solution of (36).
Iterative Solution of (36)
Initialization: Set $n = 1$ and $\mathbf{R}_{\mathbf{S}_k}^{(0)}$ which satisfies the constraints in (36).
a. Compute $\nabla_{\mathbf{R}_{\mathbf{S}_k}} g(\mathbf{R}_{\mathbf{S}_k}^{(n-1)})$ using (42), and (41).
b. Find the descent direction $\Delta\mathbf{R}_{\mathbf{S}_k}^{(n)}$, by solving the SDP problem given by (38).
c. Compute the optimal step size $\alpha_k^{(n)}$ by solving (39).
d. Update the transmit auto-correlation matrix using $\mathbf{R}_{\mathbf{S}_k}^{(n)} = \mathbf{R}_{\mathbf{S}_k}^{(n-1)} + \alpha_k^{(n)} \Delta\mathbf{R}_{\mathbf{S}_k}^{(n)}$.
e. If convergence criterion is satisfied, return. Else, set $n \leftarrow n + 1$ and go to step a.
3. Construct a signal waveform \mathbf{S}_k with auto-correlation matrix $\mathbf{R}_{\mathbf{S}_k}^{(n)}$ and obtain measurement \mathbf{X}_k .
4. Set $k \leftarrow k + 1$ and go to step 1.

conditional RMB for estimating $\boldsymbol{\theta}$ at the k th step, given previous observations, $\mathbf{X}^{(k-1)}$, is defined as

$$\Sigma_k \succeq \mathbf{C}_k^{(\text{RMB})} \triangleq \mathbf{T}(\mathbf{D}_k - \mathbf{1}_{J \times J})^{-1} \mathbf{T}^T \quad (28)$$

where the $Q \times J$ matrix $\mathbf{T} = [\mathbf{t}_1, \dots, \mathbf{t}_J]$ contains the *test points* \mathbf{t}_i , $i = 1, \dots, J$, such that $\boldsymbol{\theta} + \mathbf{t}_i \in \Theta$. The (i, j) element of the $J \times J$ matrix \mathbf{D}_k , is given by

$$\begin{aligned} [\mathbf{D}_k]_{i,j} &= \int_{\Theta} \mu_{i,j}(\boldsymbol{\theta}) \lambda_{\mathbf{t}_i, \mathbf{t}_j, \mathbf{X}^{(k-1)}}(\boldsymbol{\theta}) d\boldsymbol{\theta} \\ &\triangleq \Psi_{\mu_{i,j}}[\lambda_{\mathbf{t}_i, \mathbf{t}_j, \mathbf{X}^{(k-1)}}(\boldsymbol{\theta})] \end{aligned} \quad (29)$$

where

$$\begin{aligned} \lambda_{\mathbf{t}_i, \mathbf{t}_j, \mathbf{X}^{(k-1)}}(\boldsymbol{\theta}) &\triangleq \int_{\Omega} \mathcal{L}_k(\mathbf{X}_k, \boldsymbol{\theta} + \mathbf{t}_i, \boldsymbol{\theta}) \\ &\quad \times \mathcal{L}_k(\mathbf{X}_k, \boldsymbol{\theta} + \mathbf{t}_j, \boldsymbol{\theta}) d\mathbf{X}_k \end{aligned} \quad (30)$$

$$\mu_{i,j}(\boldsymbol{\theta}) \triangleq \frac{f_{\theta}(\boldsymbol{\theta} + \mathbf{t}_i) \mathbf{X}^{(k-1)} f_{\theta}(\boldsymbol{\theta} + \mathbf{t}_j) \mathbf{X}^{(k-1)}}{f_{\theta}(\boldsymbol{\theta} | \mathbf{X}^{(k-1)})}, \quad (31)$$

in which

$$\mathcal{L}_k(\mathbf{X}_k, \boldsymbol{\varphi}, \boldsymbol{\theta}) = \frac{f_{\mathbf{X}_k}(\mathbf{X}_k | \boldsymbol{\varphi}, \mathbf{X}^{(k-1)})}{f_{\mathbf{X}_k}(\mathbf{X}_k, |\boldsymbol{\theta}, \mathbf{X}^{(k-1)})}, \quad (32)$$

and $\Psi_{\mu_{i,j}}(\cdot)$ is a functional on \mathbb{R} , defined by

$$\Psi_{\mu_{i,j}}(g) \triangleq \int_{\Theta} g(\boldsymbol{\theta}') \mu_{i,j}(\boldsymbol{\theta}') d\boldsymbol{\theta}'. \quad (33)$$

Proof: The proof is identical to the proof of the classic RMB presented in [34], except for changing the pdfs and the expectations to be conditioned on the history observations $\mathbf{X}^{(k-1)}$. ■

In Appendix C, it is shown that under the model described in Section II, the (i, j) element of the matrix \mathbf{D}_k is given by

$$[\mathbf{D}_k]_{i,j} = \Psi_{\mu_{i,j}} \{ \exp [2L \cdot \text{tr} [\text{Re} (\mathbf{A}_k(\boldsymbol{\theta}, \mathbf{t}_i, \mathbf{t}_j) \mathbf{R}_{\mathbf{S}_k})]] \} \quad (34)$$

where

$$\begin{aligned} \mathbf{A}_k(\boldsymbol{\theta}, \mathbf{t}_i, \mathbf{t}_j) &\triangleq (\mathbf{H}_k(\boldsymbol{\theta} + \mathbf{t}_i) - \mathbf{H}_k(\boldsymbol{\theta}))^H \mathbf{R}^{-1} \\ &\quad \times (\mathbf{H}_k(\boldsymbol{\theta} + \mathbf{t}_j) - \mathbf{H}_k(\boldsymbol{\theta})). \end{aligned} \quad (35)$$

B. Waveform Optimization

We aim to find the transmit auto-correlation matrix at the k th step, which “minimizes” the RMB. As discussed in the previous section, one can consider several optimization criteria, and again, we consider the minimization of the trace of the bound with a weighting matrix. When using a sparse set of test-points, the matrix \mathbf{T} in (28) is chosen such that the bound is maximized. However, in this approach the “optimal” set of test-points depend on $\mathbf{R}_{\mathbf{S}_k}$ which needs to be determined. An alternative and efficient approach is choosing a reasonably large dense set of test points distributed over the parameter space corresponding to the major sidelobes of the ambiguity function [5], [44]. Assuming a given set of test points, \mathbf{T} , the minimization problem can be stated as

$$\begin{aligned} \bar{\mathbf{R}}_{\mathbf{S}_k} &= \arg \min_{\mathbf{R}_{\mathbf{S}_k}} \text{tr} (\mathbf{W} \mathbf{T} (\mathbf{D}_k - \mathbf{1}_{J \times J})^{-1} \mathbf{T}^T) \\ \text{s.t.} \quad &\text{tr} (\mathbf{R}_{\mathbf{S}_k}) = P, \mathbf{R}_{\mathbf{S}_k} \succeq \mathbf{0} \end{aligned} \quad (36)$$

where $\mathbf{W} = \text{diag}(w_1, \dots, w_Q)$ is a positive-definite weighting matrix. Unfortunately, this optimization problem is not convex. In the following, the *steepest descent* method [38], [41] is used to iteratively solve the above minimization problem, which in our case turns into an SDP problem.

Let g denote the objective function in (36), i.e.

$$g(\mathbf{R}_{\mathbf{S}_k}) \triangleq \text{tr} (\tilde{\mathbf{T}} (\mathbf{D}_k - \mathbf{1}_{J \times J})^{-1} \tilde{\mathbf{T}}^T) \quad (37)$$

where $\tilde{\mathbf{T}} = \mathbf{W}^{1/2} \mathbf{T}$. In general, descent methods produce a minimizing sequence $\mathbf{R}_{\mathbf{S}_k}^{(n)}$, $n = 1, 2, \dots$, having the form $\mathbf{R}_{\mathbf{S}_k}^{(n)} = \mathbf{R}_{\mathbf{S}_k}^{(n-1)} + \alpha_k^{(n)} \Delta\mathbf{R}_{\mathbf{S}_k}^{(n)}$, where $\alpha_k^{(n)} \geq 0$ and $\Delta\mathbf{R}_{\mathbf{S}_k}^{(n)}$ denotes the step size, and the *descent direction* at the n th iteration, respectively. The descent direction $\Delta\mathbf{R}_{\mathbf{S}_k}^{(n)}$, is a matrix that decreases the objective function (toward a local minimum), which satisfies $\text{Re} \langle \nabla_{\mathbf{R}_{\mathbf{S}_k}} g(\mathbf{R}_{\mathbf{S}_k}^{(n-1)}), \Delta\mathbf{R}_{\mathbf{S}_k}^{(n)} \rangle < 0$, where $\langle \cdot, \cdot \rangle$ stands for the inner product between two matrices \mathbf{A} , and \mathbf{B} , i.e. $\langle \mathbf{A}, \mathbf{B} \rangle = \text{tr} (\mathbf{A} \mathbf{B}^H)$, and $\nabla_{\mathbf{A}} g$ denotes the gradient operator of the scalar function g w.r.t. the matrix \mathbf{A} , whose (i, j) element is given by $[\nabla_{\mathbf{A}} g]_{i,j} = \frac{\partial g}{\partial \mathbf{A}_{i,j}}$.

The algorithm starts with initialization of the matrix $\mathbf{R}_{\mathbf{S}_k}^{(0)}$ satisfying the energy and semi-definite constraints, i.e. $\text{tr}(\mathbf{R}_{\mathbf{S}_k}^{(0)}) = P$, and $\mathbf{R}_{\mathbf{S}_k}^{(0)} \succeq \mathbf{0}$. Given $\mathbf{R}_{\mathbf{S}_k}^{(n-1)}$, the goal is to find a matrix $\mathbf{R}_{\mathbf{S}_k}^{(n)}$, which is closer to a local minimum of the objective function, g . The matrix $\mathbf{R}_{\mathbf{S}_k}^{(n)}$ should also satisfy the energy and semi-definite constraints. In order to find the descent direction at the n th iteration, the following minimization problem is considered [41, Ch. 3]

$$\begin{aligned} \Delta\mathbf{R}_{\mathbf{S}_k}^{(n)} &= \arg \min_{\Delta\mathbf{R}_{\mathbf{S}_k}} \text{Re} \langle \nabla_{\mathbf{R}_{\mathbf{S}_k}} g(\mathbf{R}_{\mathbf{S}_k}^{(n-1)}), \Delta\mathbf{R}_{\mathbf{S}_k} \rangle \\ \text{s.t.} \quad &\text{tr} (\Delta\mathbf{R}_{\mathbf{S}_k}) = 0, \mathbf{R}_{\mathbf{S}_k}^{(n-1)} + \Delta\mathbf{R}_{\mathbf{S}_k} \succeq \mathbf{0}. \end{aligned} \quad (38)$$

The constrained minimization in (38) is an SDP optimization problem, that can be solved efficiently. After finding the

descent direction $\Delta \mathbf{R}_{\mathbf{S}_k}^{(n)}$, we perform a *line search* to compute the step size, $\alpha_k^{(n)}$, that determines how far $\mathbf{R}_{\mathbf{S}_k}^{(n-1)}$ should move along that direction. Mathematically, the line search minimization problem is given by [38, Ch. 9.2]

$$\alpha_k^{(n)} = \arg \min_{\alpha \in \mathbb{R}_+} g \left(\mathbf{R}_{\mathbf{S}_k}^{(n-1)} + \alpha \Delta \mathbf{R}_{\mathbf{S}_k}^{(n)} \right) \quad (39)$$

where \mathbb{R}_+ denotes the space of nonnegative real numbers, and the minimization is performed for values of α that maintain $g(\mathbf{R}_{\mathbf{S}_k}^{(n-1)} + \alpha \Delta \mathbf{R}_{\mathbf{S}_k}^{(n)}) \geq 0$. After finding the optimal step size, we update $\mathbf{R}_{\mathbf{S}_k}^{(n)} = \mathbf{R}_{\mathbf{S}_k}^{(n-1)} + \alpha_k^{(n)} \Delta \mathbf{R}_{\mathbf{S}_k}^{(n)}$. Note that since the problem given in (36) is not convex, the transmit auto-correlation matrix obtained from the aforementioned linearization technique, may be a local and not global maximizer of (36). Moreover, typically to linearization techniques, the solution depends on the initial choice of the covariance matrix. However, simulations show that in our considered scenarios the algorithm is not very sensitive to the initial choice. In the simulations, a diagonal covariance matrix is chosen as an initial point.

Implementation of (38) involves computation of the gradient of the objective function g . The partial derivative of the objective function in (37) w.r.t. the (i, j) element of the matrix $\mathbf{R}_{\mathbf{S}_k}$, is given by (40), shown at the bottom of the page, where the first equality is obtained using the chain rule and the identity $\frac{d \text{tr}(\mathbf{A} \mathbf{X}^{-1} \mathbf{B})}{d \mathbf{X}} = -(\mathbf{X}^{-1} \mathbf{B} \mathbf{A} \mathbf{X}^{-1})^T$, and the second equality is obtained using the identity $\text{tr}(\mathbf{A}^T \mathbf{B}) = \text{vec}^T(\mathbf{A}) \text{vec}(\mathbf{B})$, where the operator $\text{vec}(\cdot)$ concatenates the columns of a matrix. Using (34), the (l, m) element of the matrix $\mathbf{L}_k^{(i,j)}$ is given by

$$\left[\mathbf{L}_k^{(i,j)} \right]_{l,m} = L \cdot \Psi_{\mu_{l,m}} \left\{ \exp [2L \text{tr} (\text{Re} (\mathbf{A}_k(\boldsymbol{\theta}, \mathbf{t}_l, \mathbf{t}_m) \mathbf{R}_{\mathbf{S}_k}))] \right. \\ \left. \times [\mathbf{A}_k^T(\boldsymbol{\theta}, \mathbf{t}_l, \mathbf{t}_m)]_{i,j} \right\}. \quad (41)$$

Finally, note that (40) can be written in matrix form as

$$\nabla_{\mathbf{R}_{\mathbf{S}_k}} g = - \{ \mathbf{I}_{N_T} \otimes \text{vec}^T [\mathbf{G}_k(\mathbf{R}_{\mathbf{S}_k})] \} \mathbf{L}_k(\mathbf{R}_{\mathbf{S}_k}) \quad (42)$$

where \mathbf{I}_{N_T} denotes an identity matrix of size N_T , and the (i, j) block of $\mathbf{L}_k(\mathbf{R}_{\mathbf{S}_k})$ is given by $[\mathbf{L}_k(\mathbf{R}_{\mathbf{S}_k})]_{i,j} = \text{vec}(\mathbf{L}_k^{(i,j)})$ for $i, j = 1, \dots, N_T$.

The calculation of (41) involves computation of a multivariate integral, which can be performed numerically using MC integration along with MH sampling technique similarly as in Section III-D. In summary, the steps of the waveform optimization method based on RMB at the k th step are described in Table II.

C. Computational Complexity

In this subsection, we analyze the computational complexity of the proposed waveform design technique at the k th pulse index. In the following, N_d denotes the number of iterations carried out by the steepest descent method. According to Table II, the computation complexity of the proposed algorithm is approximately equal to the summation of the following factors. Similarly to the calculation in Section III-E, the MH sampler complexity (step 1 in Table II) is approximately $Q N_s \mathcal{O}(N_R N_T L k + N_R^2 L k + N_R L k)$. The following complexity factors are attributed to step 2 in Table II. The complexity of constructing the matrix \mathbf{D}_k using MC integration is approximately equal to $N_d N_s \mathcal{O}(J^2 N_T^2 N_R + J^2 N_T^3)$ [41]. The complexity of constructing \mathbf{L}_k is approximately equal to $N_d N_s \mathcal{O}(J^2 N_T^2 N_R^2 + 2 J^2 N_T^3)$ [45] which results from matrix products and summations. The complexity of constructing the matrix \mathbf{G}_k and the gradient in (42) are approximately $N_d \mathcal{O}(J^3 + J^2 Q)$ and $N_d \mathcal{O}(N_T^3 J^4)$, respectively. Finally, the complexity of constructing the descent direction via an SDP optimization problem (step 3 in Table II) is approximately $N_d \mathcal{O}(\sqrt{\log N_T})$ [38], and the line search algorithm (step 4 in Table II) complexity is approximately $N_d \mathcal{O}(\log N_G)$, where N_G is the grid size partition of the line search [41]. In the simulations, the values of N_d and N_G are both bounded above by 10^2 . Summing up the aforementioned factors, the number of operations due to the significant factors is of order $Q N_s \mathcal{O}(N_R N_T L k + N_R^2 L k) + N_d N_s \mathcal{O}(J^2 N_T^2 N_R^2 + 2 J^2 N_T^3) + N_d \mathcal{O}(N_T^3 J^4)$.

Compared to the complexity of the BCRB waveform design technique, it can be seen that the RMB waveform design technique is much heavier. The main reason is the use of the iterative steepest descent method which adds further dimension to the complexity, as opposed to the BCRB waveform design technique.

In the next section, the superiority of the RMB-based over the BCRB-based waveform design will be demonstrated. This superiority is significant mainly for low pulse indices, and it is achieved because unlike the BCRB, the RMB is able to control the sidelobes such that the probability of large errors is reduced. As the pulse index increases, the performances of the two methods coincide. Accordingly, in such case, it is preferred to use the BCRB instead of the RMB as the optimization criterion. In practice, a criterion should be invoked to decide when the algorithm should switch from using the RMB technique to the BCRB technique.

V. NUMERICAL RESULTS

In this section, we evaluate the performance of the proposed adaptive waveform design methods via several examples and

$$\left[\nabla_{\mathbf{R}_{\mathbf{S}_k}} g \right]_{i,j} = -\text{tr} \left\{ \left[\underbrace{(\mathbf{D}_k - \mathbf{1}_{J \times J})^{-1} \tilde{\mathbf{T}}^T \tilde{\mathbf{T}} (\mathbf{D}_k - \mathbf{1}_{J \times J})^{-1}}_{\mathbf{G}_k} \right]^T \underbrace{\frac{\partial \mathbf{D}_k}{\partial [\mathbf{R}_{\mathbf{S}_k}]_{i,j}}}_{\mathbf{L}_k^{(i,j)}} \right\} = -\text{vec}^T(\mathbf{G}_k) \text{vec} \left(\mathbf{L}_k^{(i,j)} \right) \quad (40)$$

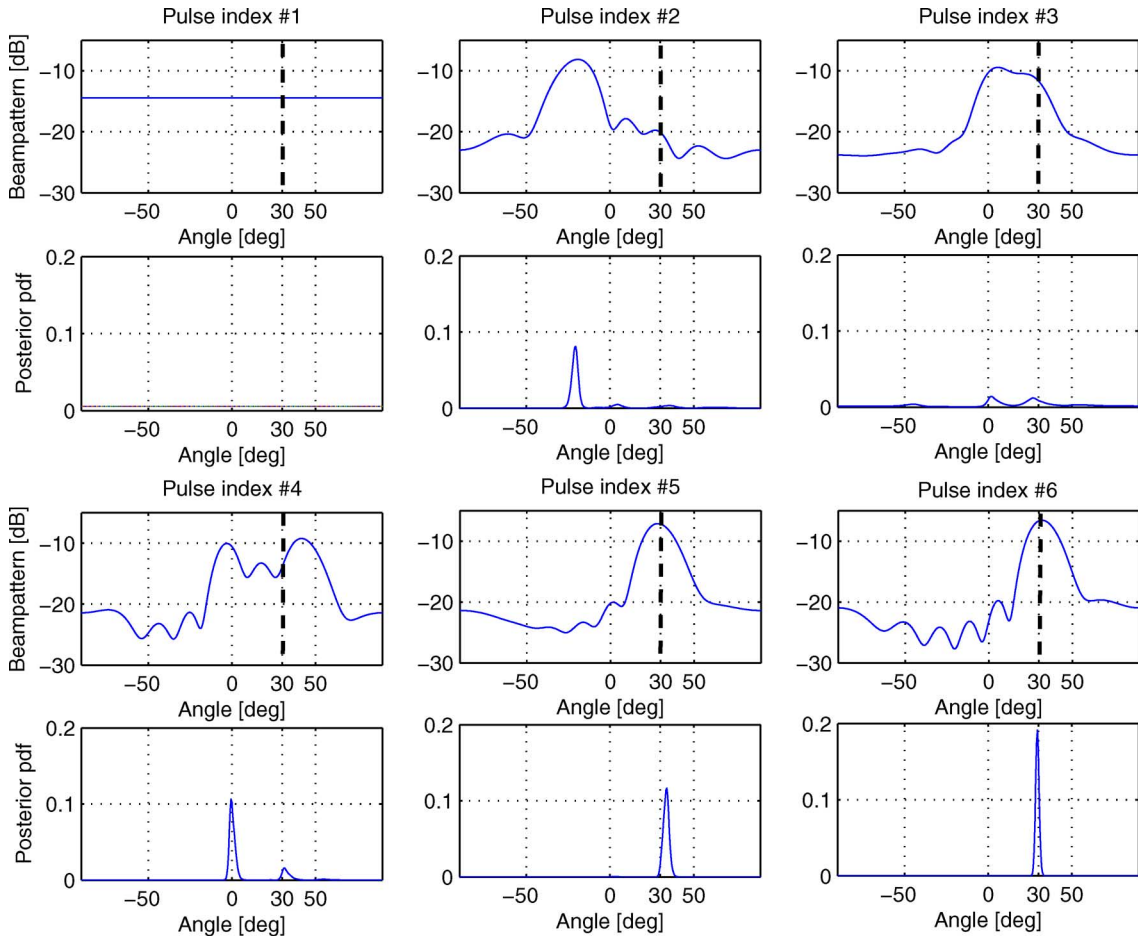


Fig. 2. Optimal transmit beampatterns (first and third rows) and posterior pdf's (second and fourth rows) versus φ for various pulse steps using BCRB waveform optimization, assuming unknown amplitude with $\varphi = 30^\circ$ and ASNR = -6 dB, using $N_R = N_T = 7$.

demonstrate their advantages compared to fixed transmit waveform, space-reversal technique [30], and transmitting sum beam steered at the MMSE estimate of the target direction.

The model presented in (2) is general and suitable for various signal processing problems. In this section, we consider a MIMO radar as a useful application. MIMO radar is an emerging technology that attracts the attention of many researchers and practitioners alike [1]–[4].

Consider a mono-static radar consisting of two co-located arrays of N_T transmitters and N_R receivers. The received signal model in the presence of M targets can be expressed as [4, Ch. 4]

$$\mathbf{x}_k(t) = \sum_{m=1}^M \alpha_m e^{-j\omega_{D_m} k} \mathbf{a}_R(\varphi_m) \mathbf{a}_T^T(\varphi_m) \mathbf{s}_k(t - \tau_m) + \mathbf{n}_k(t), \quad t \in [0, T_0] \quad (43)$$

where $\{\alpha_m, \varphi_m, \tau_m, \omega_{D_m}\}$ are the complex attenuation, direction, propagation delay, and Doppler frequency shift of the m th target, respectively, and $\mathbf{a}_R(\cdot) \in \mathbb{C}^{N_R \times 1}$, $\mathbf{a}_T(\cdot) \in \mathbb{C}^{N_T \times 1}$ are the steering vectors for the receive and transmit arrays, respectively. In case of known propagation delay, it can be readily seen that the l th sample of the data model in (43) is identical to the model given in (1), and thus the proposed waveform design methods can be used. The case of unknown range/delay

can also be treated using the techniques described in this paper, since the delay is a linear operation. In particular, the model in (43) in the frequency domain can be expressed as the model in (1). In the simulation study, we consider a signal model with known range-Doppler, which can be expressed as [2]

$$\mathbf{X}_k = \underbrace{\sum_{m=1}^M \alpha_m \mathbf{a}_R(\varphi_m) \mathbf{a}_T^T(\varphi_m)}_{\mathbf{H}} \mathbf{S}_k + \mathbf{N}_k. \quad (44)$$

The receive and transmit arrays are uniform and linear with $N_R = N_T = 7$ elements, with half wavelength inter-element spacing for both transmit and receive arrays, and $\mathbf{R} = \sigma^2 \mathbf{I}_{N_R}$. The transmit beamwidth in the considered scenario is approximately 34° . In the simulations, we consider a uniform *a-priori* distribution for the targets directions, i.e. $\varphi_m \sim U(-\frac{\pi}{2}, \frac{\pi}{2})$ for $1 \leq m \leq M$. Notice that the BCRB does not exist for uniform prior distribution since the regularity conditions are not satisfied. Accordingly, we assume that J_{P_0} is constant over $(-\frac{\pi}{2}, \frac{\pi}{2})$, which is an artificial, but reasonable assumption. Also, we consider a circular complex Gaussian *a-priori* distribution with zero mean and variance $\sigma_{\alpha_m}^2$ for the targets complex amplitudes, i.e. $\alpha_m \sim \mathcal{N}^c(0, \sigma_{\alpha_m}^2)$ for $1 \leq m \leq M$. In the simulations, the values of $\{\sigma_{\alpha_m}^2\}_{m=1}^M$ are chosen to be arbitrarily large reflecting lack of prior statistical information on the amplitudes. The elements of the unknown vector parameter $\boldsymbol{\theta} =$

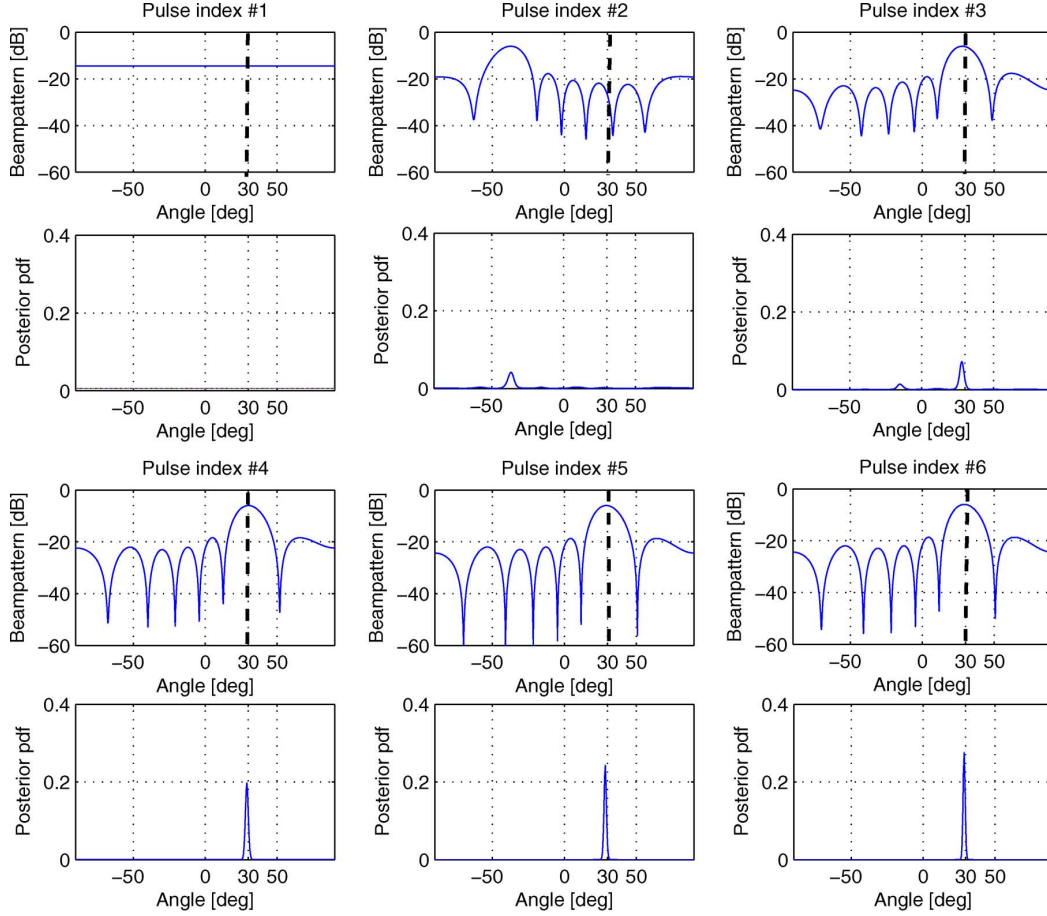


Fig. 3. Optimal transmit beampatterns (first and third rows) and posterior pdf's (second and fourth rows) versus φ for various pulse steps using RMB waveform optimization, assuming unknown amplitude with $\varphi = 30^\circ$ and $\text{ASNR} = -6$ dB, using $N_R = N_T = 7$.

$[\varphi^T, \text{Re}(\alpha^T), \text{Im}(\alpha^T)]^T$ where $\varphi = [\varphi_1, \dots, \varphi_M]^T$ and $\alpha = [\alpha_1, \dots, \alpha_M]^T$, are considered to be statistically independent.

A. Single Target

In this subsection, we consider waveform optimization in the presence of single target ($M = 1$), with unknown angle φ and unknown complex amplitude α . In this case, the unknown vector parameter is $\theta = [\varphi, \text{Re}(\alpha), \text{Im}(\alpha)]^T$. In the minimization problem (22), we choose $w_1 = 1/\text{rad}^2$ and $w_2 = w_3 = 1$. In the simulations, we assume that the target is located at unknown direction $\varphi = 30^\circ$ with array signal-to-noise ratio (ASNR) defined as $\text{ASNR} \triangleq |\alpha|^2 P N_R L / \sigma^2 = -6$ dB.

Figs. 2 and 3 show the optimized transmit beampatterns (first and third rows), defined as $G_{T_k}(\varphi) \triangleq \mathbf{a}_T^H(\varphi) \mathbf{R}_{S_k}^* \mathbf{a}_T(\varphi)$, and the posterior pdf's (second and fourth rows), as a function of φ and pulse index, using the BCRB and RMB based waveform design methods, respectively. It can be seen that as the pulse index increases, the beampattern peak location appears closer to the target direction, as expected, and the posterior pdf's become focused with reduced spread, which implies better estimation performance. Also, it is evident that at least for the first pulse iterations, the RMB-based waveform design technique better focuses on the target direction, compared to the BCRB-based waveform design technique. These figures illustrate the auto-focusing capability of the proposed adaptive waveform design techniques.

In the next examples, we evaluate and compare the estimation performance of the following waveform design methods; (1) fixed uncorrelated waveforms, i.e. $\mathbf{R}_{S_k} = (P/N_T) \mathbf{I}_{N_T}$, (2) space-reversal technique [30], where as each pulse index the conjugate of the received signal is transmitted (with power normalization), (3) transmitting sum-beam steered at the MMSE estimate of the target direction, i.e. $\mathbf{R}_{S_k} = \frac{P}{N_T} \mathbf{a}_T^*(\hat{\varphi}_{k-1}) \mathbf{a}_T^T(\hat{\varphi}_{k-1})$, where $\hat{\varphi}_{k-1} = \text{E}(\varphi | \mathbf{X}^{(k-1)})$ is the MMSE estimator of φ at the k th pulse index based on $\mathbf{X}^{(k-1)}$, and the proposed adaptive waveform design methods based on (4) BCRB and (5) RMB. In order to estimate the parameter of interest φ , the root mean-square-error (RMSE) of the MMSE estimator is evaluated using 500 independent trials. Fig. 4 presents the RMSE for estimation of φ using the above methods as a function of the pulse index for $\text{ASNR} = -6$ dB. It can be seen that the proposed waveform design techniques result in significantly better performance compared to the other tested methods. Also, in accordance to the previous figures, slightly better results for the RMB-based waveform design technique is evident, compared to the BCRB-based waveform design technique, for the first pulse iterations. Note that the relatively good performance obtained with $\text{ASNR} = -6$ dB is due to the increase of the *effective* SNR achieved by integration over several pulses, and due to the array gain at the transmitter. The SNR increase due to 6 pulses is about 7.8 dB, and assuming a focused beam during all these pulses, the array gain is about

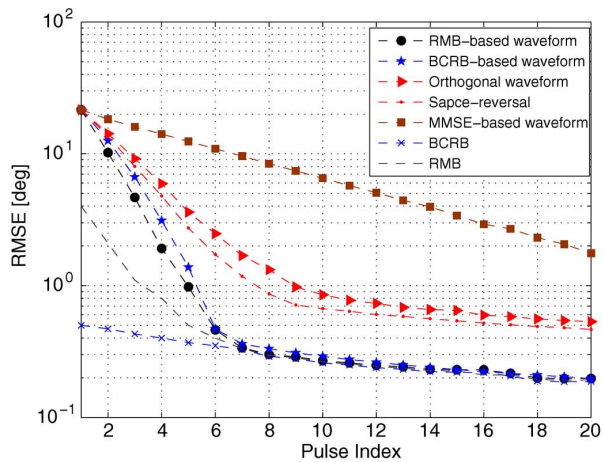


Fig. 4. RMSE versus pulse index, with ASNR = -6 dB, using $N_R = N_T = 7$.

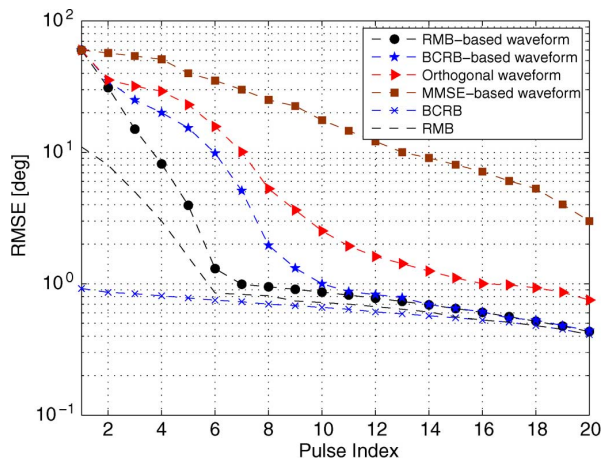


Fig. 5. RMSE versus pulse index, with ASNR = -6 dB, using $N_R = 2$ and $N_T = 7$.

8.4 dB. This means that the total effective SNR after 6 pulses is about 10.2 dB, which allows reasonable estimation accuracy. However, before the target is detected, its location is unknown to the transmitter and therefore, in practice, it cannot perfectly focus its beams toward the target. The proposed approach allows earning part of the transmit array gain before the target is detected, and in fact performs beamforming-before-detect (BBD) in an adaptive manner.

In order to illustrate the advantage of using the RMB upon the BCRB for waveform design, we will consider another array configuration with ambiguity nature in which the receive and transmit arrays are uniform and linear with $N_T = 2$ and $N_R = 7$ elements, with half wavelength inter-element spacing for the transmit array and three wavelength inter-element spacing for the receive array. Fig. 5 presents the RMSE for estimation of φ as a function of the pulse index for ASNR = -6 dB. Note that the RMSE for the space-reversal technique is not presented, since it can not be applied in case of different number of elements in the transmit and receive arrays. It can be seen that the RMB-based waveform design technique results in significantly better performance compared to the other methods. Fig. 6 presents the RMSE for estimation of φ as a function of the ASNR at pulse index $k = 6$. This figure shows that by using

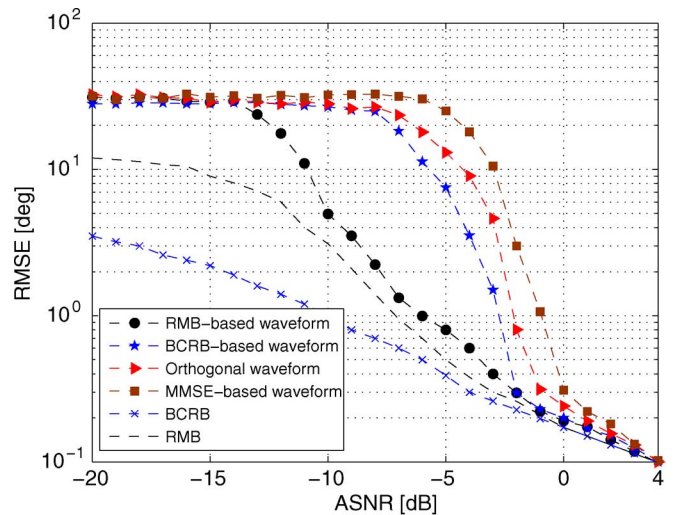


Fig. 6. RMSE versus ASNR, at $k = 6$ pulse index, using $N_R = 2$ and $N_T = 7$.

the RMB-based waveform design technique, the threshold SNR is significantly lower compared to BCRB-based waveform design technique and to the other methods. This improvement is obtained since the RMB takes into account the contribution of large errors due to sidelobes in the posterior function, and therefore, it is capable to control the sidelobes, while, the BCRB ignores the contribution of these sidelobes, and may result in waveforms with high ambiguity level. Figs. 7 and 8 show the optimized transmit beampatterns (first and third rows), and the posterior pdf's (second and fourth rows), as a function of φ and pulse index, using the BCRB and RMB based waveform design methods, respectively. These figures are consistent with the previous figure.

B. Two Targets

In this subsection, we consider waveform optimization for two targets ($M = 2$), assuming unknown angles φ_1 and φ_2 with unknown complex amplitudes α_1 and α_2 , respectively. In the minimization problem stated in (22), we choose $w_1 = w_2 = 1/\text{rad}^2$ and $w_l = 1$ for $l = 3, \dots, 6$. In the simulations, we assume that the targets are located at unknown directions $\varphi_1 = -10^\circ$, and $\varphi_2 = 20^\circ$, amplitudes satisfying $|\alpha_1| > |\alpha_2|$ with an overall ASNR = -6 dB.

Fig. 9 shows the optimal transmit beampattern, under BCRB and RMB criteria, as a function of φ for various pulse indices. Again, this figure illustrates the auto-focusing capability of the proposed waveform design methods also in case of multiple targets. Also, it can be seen that the proposed algorithms allocate more energy toward the direction of the second target, which is weaker. This feature is desirable, since according to the objective function, the parameters of both targets are of interest.

C. Computation Time

Fig. 10 compares the computation time between the BCRB and RMB based waveform design techniques, under the scenario considered in Fig. 2. The processing time is obtained by running the algorithms using Matlab on a 3.8 GHz Intel core i7 3930 K processor and memory of 8 GB 1600 MHz DDR3. It can be seen that the computational complexity of the waveform

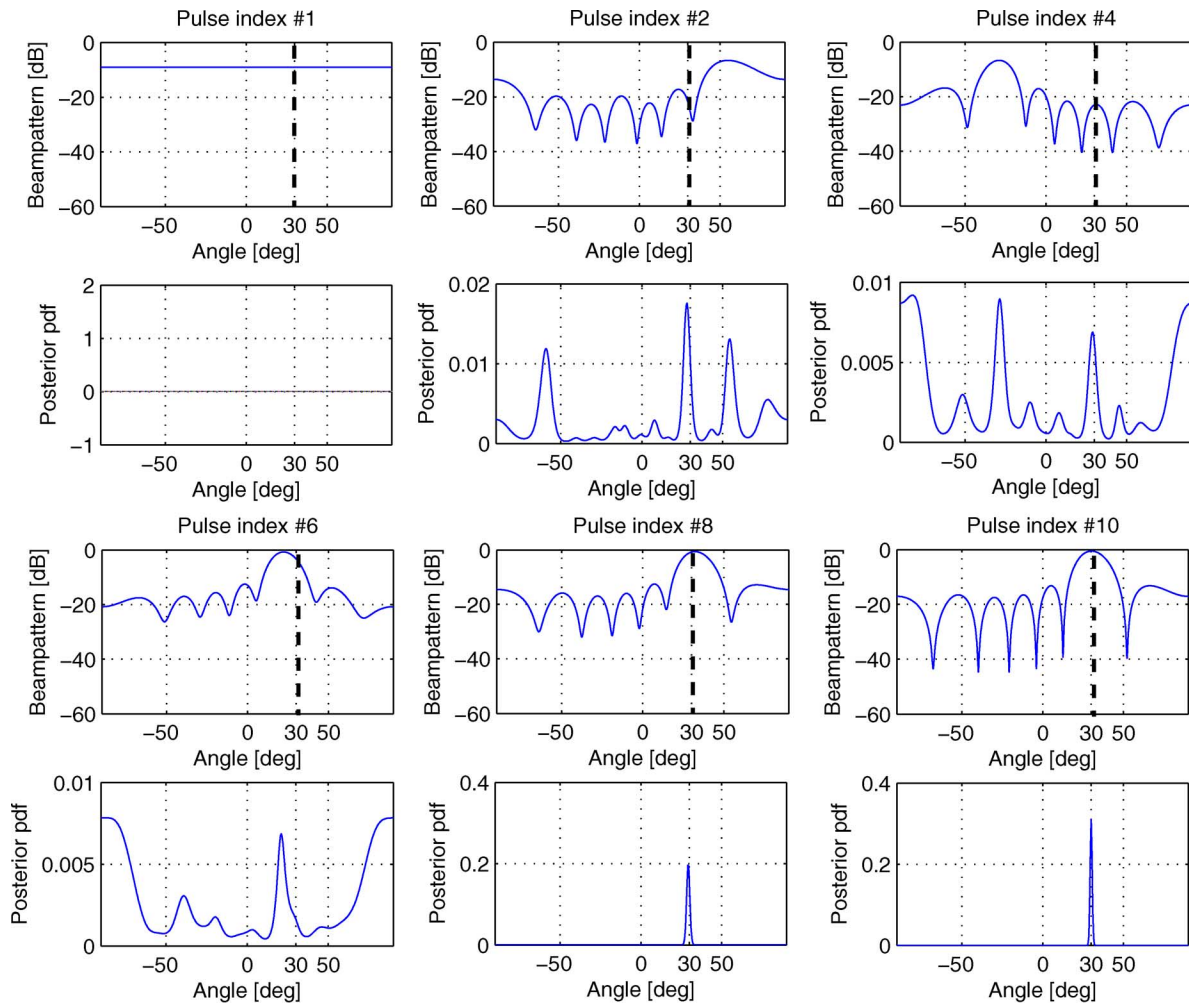


Fig. 7. Optimal transmit beampatterns (first and third rows) and posterior pdf's (second and fourth rows) versus φ for various pulse steps using BCRB waveform optimization, assuming unknown amplitude with $\varphi = 30^\circ$ and $\text{ASNR} = -6$ dB, using $N_R = 2$ and $N_T = 7$.

design technique based on the RMB criterion is higher compared to the BCRB criterion, which is consistent with the computational complexity analysis performed in Sections III-E and IV-C. For practical purposes the computation time for both algorithms is in the order of typical values of the pulse repetition time used in typical surveillance radar systems.

VI. CONCLUSION

In this paper, we proposed new techniques for adaptive waveform optimization. Instead of transmission of identical waveforms, in the proposed techniques, the waveform is determined at each step, in order to minimize the BCRB or the RMB for system parameters estimation w.r.t. the transmit/input waveform. The proposed techniques were tested via simulations for adaptive spatial transmit waveform design in the presence of single and multiple targets with a very weak ASNR. The simulations show that the proposed techniques enable a significantly higher rate of reduction in the RMSE, compared to other waveform transmission techniques.

The waveform design methods described in this paper, refer to any time-varying linear system in which the input signal can be controlled. Accordingly, it can be used for adaptive

space-time waveform design for MIMO radar. The simulations in this paper assumed known range and Doppler information. Further research can focus on performance analysis of the proposed method without prior knowledge of range and Doppler information.

Finally, in case of moving target in which the target location/parameters vary with k , the algorithm should be modified in order to consider the dynamics of the unknown parameters with some prior distribution on the change rate of the parameters. In the proposed techniques, the prior distribution at each step is taken as the posterior distribution from the previous step. In the presence of moving target, at each step, the prior distribution should be modified to take into account the uncertainties due to the dynamics of the target. Thus, by using well-known tracking methods, the proposed algorithm can be readily extended to cover also dynamic scenarios.

APPENDIX A DERIVATION OF EQUATION (19)

Using the expression for the FIM in case of deterministic signal in Gaussian noise [33], and applying the law of total

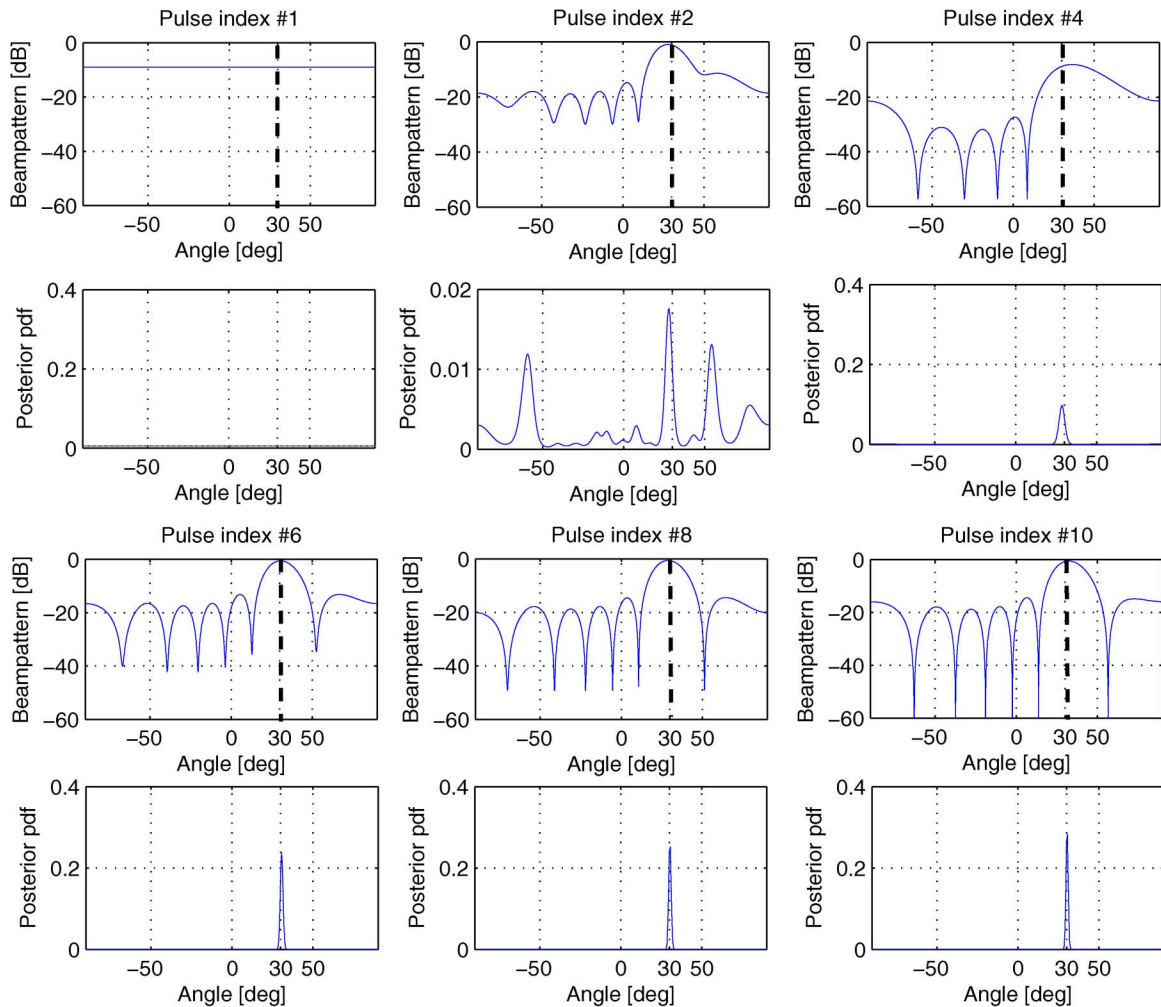


Fig. 8. Optimal transmit beampatterns (first and third rows) and posterior pdf's (second and fourth rows) versus φ for various pulse steps using RMB waveform optimization, assuming unknown amplitude with $\varphi = 30^\circ$ and $\text{ASNR} = -6$ dB, using $N_R = 2$ and $N_T = 7$.

expectation, the (i, j) element of the matrix $\Delta \mathbf{J}_{D_k}$, defined in (9), for the data model presented in (2), can be expressed as

$$[\Delta \mathbf{J}_{D_k}]_{i,j} = 2LE \left\{ \text{Re} \left[\text{tr} \left(\dot{\mathbf{H}}_{i,k}^H \mathbf{R}^{-1} \dot{\mathbf{H}}_{j,k} \mathbf{R}_{S_k} \right) | \mathbf{X}^{(k-1)} \right] \right\}, \quad (45)$$

where $\dot{\mathbf{H}}_{i,k} \triangleq \frac{\partial \mathbf{H}_k}{\partial \theta_i}$ and

$$\dot{\mathbf{H}}_k \triangleq (\dot{\mathbf{H}}_{1,k}, \dots, \dot{\mathbf{H}}_{Q,k}); \quad \mathbf{U}_i \triangleq \begin{pmatrix} \mathbf{0}_{(i-1)N_T \times N_T} & \\ & \mathbf{I}_{N_T} \\ & & \mathbf{0}_{(Q-i)N_T \times N_T} \end{pmatrix}. \quad (46)$$

Then the matrix $\dot{\mathbf{H}}_{i,k}$ can be expressed as

$$\dot{\mathbf{H}}_{i,k} = \dot{\mathbf{H}}_k \mathbf{U}_i. \quad (47)$$

Using (47), (45) can be rewritten as

$$[\Delta \mathbf{J}_{D_k}]_{i,j} = 2L \times E \left\{ \text{Re} \left[\text{tr} \left(\dot{\mathbf{H}}_k^H \mathbf{R}^{-1} \dot{\mathbf{H}}_k \mathbf{U}_j \mathbf{R}_{S_k} \mathbf{U}_i^H \right) | \mathbf{X}^{(k-1)} \right] \right\}. \quad (48)$$

The matrix \mathbf{U}_i can be represented by a combination of unit vectors in the following form

$$\mathbf{U}_i = \sum_{m=(i-1)N_T+1}^{iN_T} \tilde{\mathbf{e}}_m \mathbf{e}_{m-(i-1)N_T}^T, \quad (49)$$

where $\tilde{\mathbf{e}}_m$ and \mathbf{e}_m denote the m th column of the identity matrix of dimensions $N_T Q$ and N_T , respectively. By denoting $\alpha_i = (i-1)N_T$, substituting (49) in (48), and using the linearity of the trace and real operators, one obtains (50), shown at the bottom of the following page, where the last equality follows from the definitions of $\tilde{\mathbf{e}}_m$ and \mathbf{e}_m , and by denoting $\tilde{n} = n - (i-1)N_T$, $\tilde{m} = m - (j-1)N_T$. Equation (50) can be interpreted as taking non-overlap $N_T \times N_T$ blocks from the matrix $E(\dot{\mathbf{H}}_k^H \mathbf{R}^{-1} \dot{\mathbf{H}}_k | \mathbf{X}^{(k-1)})$, then multiplying each entry by the corresponding entry of \mathbf{R}_{S_k} (Hadamard product), and finally summing all the entries of the obtained matrix. In order to derive a closed-form expression for the IBFI, let us define

$$\mathbf{Q}_I \triangleq \mathbf{I}_Q \otimes \mathbf{1}_{1 \times N_T}. \quad (51)$$

Using (50) and (51), simple algebraic steps reveals that the IBFI can be written as (19).

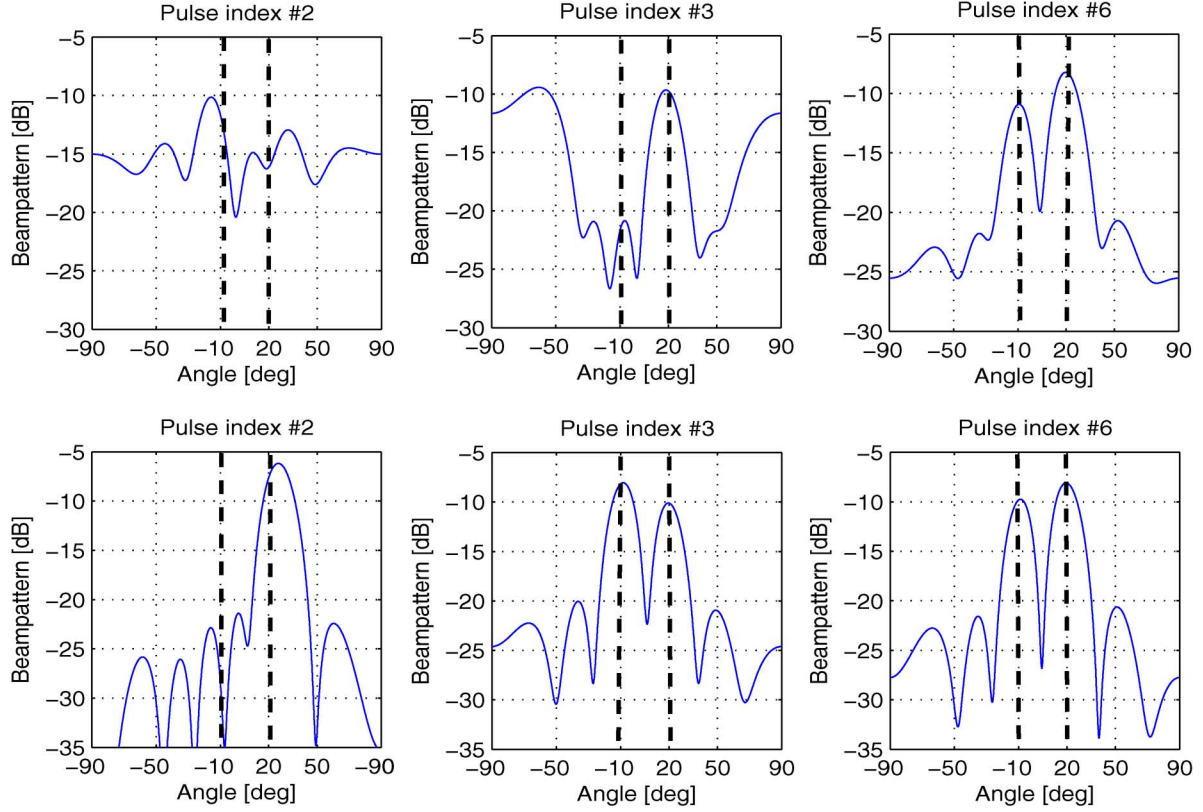


Fig. 9. Transmit beampatterns versus φ for various pulse steps using BCRB (first row) and RMB (second row) waveform optimizations, assuming unknown amplitudes with $\varphi_1 = -10^\circ$, $\varphi_2 = 20^\circ$, $|\alpha_1| > |\alpha_2|$, and ASNR = -6 dB, using $N_R = N_T = 7$.

APPENDIX B DERIVATION OF EQUATION (23)

Using Bayes theorem, the posterior pdf $f_{\boldsymbol{\theta}|\mathbf{X}^{(k-1)}}$ can be written as

$$f_{\boldsymbol{\theta}|\mathbf{X}^{(k-1)}} = f_{\boldsymbol{\theta}|\mathbf{X}^{(k-2)}} \frac{f_{\mathbf{X}_{k-1}|\mathbf{X}^{(k-2)}, \boldsymbol{\theta}}}{f_{\mathbf{X}_{k-1}|\mathbf{X}^{(k-2)}}} \quad (52)$$

$$= \frac{1}{\tilde{C}} \left(\prod_{m=1}^{k-1} f_{\mathbf{X}_m|\mathbf{X}^{(m-1)}, \boldsymbol{\theta}} \right) f_{\boldsymbol{\theta}} \quad (53)$$

where \tilde{C} is a normalization constant, independent of $\boldsymbol{\theta}$. Hence, according to (10) and using (53), the (i, j) element of the matrix $\mathbf{J}_{P_{k-1}}$ can be written as

$$\begin{aligned} [\mathbf{J}_{P_{k-1}}]_{i,j} &= -\mathbb{E} \left(\frac{\partial^2 \log f_{\boldsymbol{\theta}|\mathbf{X}^{(k-1)}}}{\partial \theta_i \partial \theta_j} \middle| \mathbf{X}^{(k-1)} \right) \\ &= -\sum_{m=1}^{k-1} \mathbb{E} \left(\frac{\partial^2 \log f_{\mathbf{X}_m|\mathbf{X}^{(m-1)}, \boldsymbol{\theta}}}{\partial \theta_i \partial \theta_j} \middle| \mathbf{X}^{(k-1)} \right) \\ &\quad - \mathbb{E} \left(\frac{\partial^2 \log f_{\boldsymbol{\theta}}}{\partial \theta_i \partial \theta_j} \middle| \mathbf{X}^{(k-1)} \right) \end{aligned}$$

$$\begin{aligned} [\Delta \mathbf{J}_{D_k}]_{i,j} &= 2LE \left\{ \text{Re} \left[\text{tr} \left(\hat{\mathbf{H}}_k^H \mathbf{R}^{-1} \hat{\mathbf{H}}_k \sum_{m=\alpha_j+1}^{\alpha_j+N_T} \tilde{\mathbf{e}}_m \mathbf{e}_{m-(j-1)N_T}^T \mathbf{R} \mathbf{s}_k \sum_{n=\alpha_i+1}^{\alpha_i+N_T} \mathbf{e}_{n-(i-1)N_T} \tilde{\mathbf{e}}_n^T \right) \middle| \mathbf{X}^{(k-1)} \right] \right\} \\ &= 2L \sum_{m=\alpha_j+1}^{\alpha_j+N_T} \sum_{n=\alpha_i+1}^{\alpha_i+N_T} \text{Re} \left\{ \text{tr} \left[\mathbb{E} \left(\hat{\mathbf{H}}_k^H \mathbf{R}^{-1} \hat{\mathbf{H}}_k \middle| \mathbf{X}^{(k-1)} \right) \tilde{\mathbf{e}}_m \mathbf{e}_{m-(j-1)N_T}^T \mathbf{R} \mathbf{s}_k \mathbf{e}_{n-(i-1)N_T} \tilde{\mathbf{e}}_n^T \right] \right\} \\ &= 2L \sum_{m=\alpha_j+1}^{\alpha_j+N_T} \sum_{n=\alpha_i+1}^{\alpha_i+N_T} \text{Re} \left\{ \left[\tilde{\mathbf{e}}_n^T \mathbb{E} \left(\hat{\mathbf{H}}_k^H \mathbf{R}^{-1} \hat{\mathbf{H}}_k \middle| \mathbf{X}^{(k-1)} \right) \tilde{\mathbf{e}}_m \right] \left[\mathbf{e}_{m-(j-1)N_T}^T \mathbf{R} \mathbf{s}_k \mathbf{e}_{n-(i-1)N_T} \right] \right\} \\ &= 2L \text{Re} \left\{ \left(\sum_{m=\alpha_j+1}^{\alpha_j+N_T} \sum_{n=\alpha_i+1}^{\alpha_i+N_T} \left[\mathbb{E} \left(\hat{\mathbf{H}}_k^H \mathbf{R}^{-1} \hat{\mathbf{H}}_k \middle| \mathbf{X}^{(k-1)} \right) \right]_{n,m} [\mathbf{R} \mathbf{s}_k]_{\tilde{m}, \tilde{n}} \right) \right\} \quad (50) \end{aligned}$$

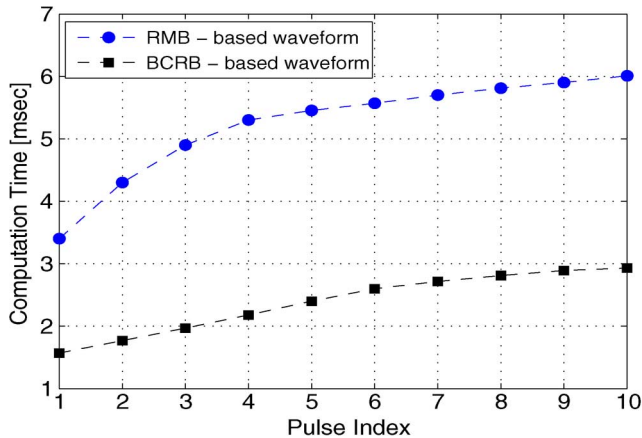


Fig. 10. Computation time versus pulse index using BCRB and RMB waveform design techniques.

$$\begin{aligned}
&= 2L \sum_{m=1}^{k-1} \text{Re} \left\{ \text{E} \left[\text{tr} \left(\dot{\mathbf{H}}_{i,m}^H \mathbf{R}^{-1} \dot{\mathbf{H}}_{j,m} \mathbf{R} \mathbf{S}_m \right) \right. \right. \\
&\quad \left. \left. \left| \mathbf{X}^{(k-1)} \right] \right\} \\
&\quad - 2 \sum_{m=1}^{k-1} \text{Re} \left\{ \text{E} \left[\text{tr} \left((\mathbf{X}_m - \mathbf{H}_k \mathbf{S}_m)^H \ddot{\mathbf{H}}_{i,j,m} \mathbf{S}_m \right) \right. \right. \\
&\quad \left. \left. \left| \mathbf{X}^{(k-1)} \right] \right\} \\
&\quad - \text{E} \left(\left. \frac{\partial^2 \log f_{\boldsymbol{\theta}}}{\partial \theta_i \partial \theta_j} \right| \mathbf{X}^{(k-1)} \right) \quad (54)
\end{aligned}$$

where the last equality reveals simply after calculating the term $\frac{\partial^2 \log f_{\mathbf{x}_m | \mathbf{x}^{(m-1)}, \boldsymbol{\theta}}}{\partial \theta_i \partial \theta_j}$. In accordance to the matrix representation given by (19), (54) can be written in matrix form as

$$\begin{aligned}
\mathbf{J}_{P_{k-1}} &= \mathbf{J}_{N_{k-1}} + \mathbf{J}_{I_{k-1}} \\
&\quad + 2L \sum_{m=1}^{k-1} \text{Re} \left\{ \mathbf{Q}_I \left[\tilde{\mathbf{\Gamma}}_m \left(\mathbf{X}^{(k-1)} \right) \right. \right. \\
&\quad \left. \left. \odot \left(\mathbf{1}_{Q \times Q} \otimes \mathbf{R}_{S_m}^T \right) \right] \mathbf{Q}_I^T \right\} \quad (55)
\end{aligned}$$

where the (i, j) element of the matrix $\mathbf{J}_{I_{k-1}}$ is given by

$$[\mathbf{J}_{I_{k-1}}]_{i,j} \triangleq -\text{E} \left(\left. \frac{\partial^2 \log f_{\boldsymbol{\theta}}}{\partial \theta_i \partial \theta_j} \right| \mathbf{X}^{(k-1)} \right), \quad (56)$$

and the (i, j) element of the matrix $\mathbf{J}_{N_{k-1}}$ is given by

$$\begin{aligned}
&[\mathbf{J}_{N_{k-1}}]_{i,j} \\
&= -2 \sum_{m=1}^{k-1} \text{Re} \left\{ \text{E} \left[\text{tr} \left((\mathbf{X}_m - \mathbf{H}_k \mathbf{S}_m)^H \ddot{\mathbf{H}}_{i,j,m} \mathbf{S}_m \right) \right. \right. \\
&\quad \left. \left. \left| \mathbf{X}^{(k-1)} \right] \right\} \quad (57)
\end{aligned}$$

where $\ddot{\mathbf{H}}_{i,j,m}(\boldsymbol{\theta}) \triangleq \frac{\partial^2 \mathbf{H}_m(\boldsymbol{\theta})}{\partial \theta_i \partial \theta_j}$.

APPENDIX C

DERIVATION OF EQUATION (34)

Under the statistics and model assumptions described in Section II, it can be concluded that $(\mathbf{X}_k | (\boldsymbol{\theta} + \mathbf{h}_i), \mathbf{X}^{(k-1)}) \sim \mathcal{N}^c(\mathbf{H}_k(\boldsymbol{\theta} + \mathbf{h}_i) \mathbf{S}_k, (\mathbf{X}^{(k-1)} \mathbf{R})$. Let $r_{\boldsymbol{\theta} + \mathbf{h}_i} \triangleq f_{\mathbf{X}_k | \mathbf{X}^{(k-1)}, (\boldsymbol{\theta} + \mathbf{h}_i)}$. The integrand of $\lambda_{t_i, t_j, \mathbf{X}^{(k-1)}}(\boldsymbol{\theta})$ in (30) can be expressed as

$$\begin{aligned}
\frac{r_{\boldsymbol{\theta} + \mathbf{h}_i} r_{\boldsymbol{\theta} + \mathbf{h}_j}}{r_{\boldsymbol{\theta}}} &= \beta \cdot \exp \left\{ -\text{tr} \left[(\mathbf{X}_k - \mathbf{B}_{i,j,k}(\boldsymbol{\theta}))^H \mathbf{R}^{-1} \right. \right. \\
&\quad \left. \left. \times (\mathbf{X}_k - \mathbf{B}_{i,j,k}(\boldsymbol{\theta})) \right] \right\} \cdot \exp(\vartheta_{i,j}(\boldsymbol{\theta})) \quad (58)
\end{aligned}$$

in which

$$\mathbf{B}_{i,j,k}(\boldsymbol{\theta}) = \mathbf{H}_k(\boldsymbol{\theta} + \mathbf{h}_i) + \mathbf{H}_k(\boldsymbol{\theta} + \mathbf{h}_j) - \mathbf{H}_k(\boldsymbol{\theta}) \quad (59)$$

$$\vartheta_{i,j}(\boldsymbol{\theta}) = 2L \cdot \text{tr} [\text{Re} (\mathbf{A}_k(\boldsymbol{\theta}, \mathbf{h}_i, \mathbf{h}_j) \mathbf{R}_{S_k})] \quad (60)$$

where β is a normalization constant. The integral of the left exponential term (and the constant β) in (58) over Ω , is equal to one (follows from the integral of pdf over the entire space). Therefore, we obtain

$$\lambda_{t_i, t_j, \mathbf{X}^{(k-1)}}(\boldsymbol{\theta}) = \exp(\vartheta_{i,j}(\boldsymbol{\theta})), \quad (61)$$

and according to (29), $[\mathbf{D}_k]_{i,j}$ is given by

$$\begin{aligned}
[\mathbf{D}_k]_{i,j} &= \Psi_{\mu_{i,j}} \left[\lambda_{t_i, t_j, \mathbf{X}^{(k-1)}}(\boldsymbol{\theta}) \right] \\
&= \Psi_{\mu_{i,j}} \left[\exp(\vartheta_{i,j}(\boldsymbol{\theta})) \right] \\
&= \Psi_{\mu_{i,j}} \left[\exp \left\{ 2L \cdot \text{tr} [\text{Re} (\mathbf{A}_k(\boldsymbol{\theta}, \mathbf{h}_i, \mathbf{h}_j) \mathbf{R}_{S_k})] \right\} \right]. \quad (62)
\end{aligned}$$

REFERENCES

- [1] I. Bekkerman and J. Tabrikian, "Spatially coded signal model for active arrays," in *Proc. ICASSP*, May 2004, vol. 2, pp. 209–212.
- [2] I. Bekkerman and J. Tabrikian, "Target detection and localization using MIMO radars and sonars," *IEEE Trans. Signal Process.*, vol. 54, no. 10, pp. 3873–3883, Oct. 2006.
- [3] E. Fishler, A. Haimovich, R. Blum, L. Cimini, D. Chizhik, and R. Valenzuela, "Spatial diversity in radars—Models and detection performance," *IEEE Trans. Signal Process.*, vol. 54, no. 3, pp. 823–838, Mar. 2006.
- [4] J. Li and P. Stoica, *MIMO Radar Signal Process.* Hoboken, NJ: John Wiley & Sons, 2009.
- [5] J. Tabrikian, "Barankin bounds for target localization for MIMO radars," in *Proc. SAM*, Jul. 2006, pp. 278–281.
- [6] K. W. Forsythe and D. W. Bliss, "Waveform correlation and optimization issues for MIMO radar," in *Proc. 39th Asilomar Conf. Signals, Syst. Comput.*, Pacific Grove, CA, Nov. 2005, pp. 1306–1310.
- [7] J. Li, L. Xu, P. Stoica, K. W. Forsythe, and D. W. Bliss, "Range compression and waveform optimization for MIMO radar: A Cramér-Rao bound based study," *IEEE Trans. Signal Process.*, vol. 56, no. 1, pp. 218–232, Jan. 2008.
- [8] Y. Yang and R. S. Blum, "MIMO radar waveform design based on mutual information and minimum mean-square error estimation," *IEEE Trans. Aerosp. Electron. Syst.*, vol. 43, no. 1, pp. 330–343, Jan. 2007.
- [9] M. R. Bell, "Information theory and radar waveform," *IEEE Trans. Inf. Theory*, vol. 39, no. 5, pp. 1578–1597, Sep. 1993.
- [10] A. Leshem, O. Napporstek, and A. Nehorai, "Information theoretic adaptive radar waveform design for multiple extended targets," *IEEE Trans. Signal Process.*, vol. 1, no. 1, pp. 803–806, Jun. 2007.
- [11] A. De Maio and M. Lops, "Design principles of MIMO radar detectors," *IEEE Trans. Aerosp. Electron. Syst.*, vol. 43, no. 1, pp. 886–898, Jul. 2007.
- [12] B. Friedlander, "Waveform design for MIMO radar," *IEEE Trans. Aerosp. Electron. Syst.*, vol. 43, no. 1, pp. 1227–1238, Jul. 2007.

- [13] P. Stoica, J. Li, and Y. Xie, "On probing signal design for MIMO radar," *IEEE Trans. Signal Process.*, vol. 55, no. 8, pp. 4151–4161, Aug. 2007.
- [14] Y. Yang and R. S. Blum, "Minimax robust MIMO radar waveform design," *IEEE J. Sel. Topics Signal Process.*, vol. 1, no. 1, pp. 147–155, Jun. 2007.
- [15] D. R. Fuhrmann and G. San Antonio, "Transmit beamforming for MIMO radar systems using signal cross-correlation," *IEEE Trans. Aerosp. Electron. Syst.*, vol. 44, no. 1, pp. 1–16, Jan. 2008.
- [16] J. Li, P. Stoica, and X. Zheng, "Signal synthesis and receiver design for MIMO radar imaging," *IEEE Trans. Signal Process.*, vol. 56, no. 8, pp. 3959–3968, Aug. 2008.
- [17] C. Y. Chen and P. P. Vaidyanathan, "MIMO radar waveform optimization with prior information of the extended target and clutter," *IEEE Trans. Signal Process.*, vol. 57, no. 9, pp. 3533–3544, Sep. 2009.
- [18] B. Tang, J. Tang, and Y. Peng, "MIMO radar waveform design in colored noise based on information theory," *IEEE Trans. Signal Process.*, vol. 58, no. 9, pp. 4684–4697, Sep. 2010.
- [19] T. Naghibi, M. Namvar, and F. Behina, "Optimal and robust waveform design for MIMO radars in the presence of clutter," *IEEE Trans. Signal Process.*, vol. 90, no. 4, pp. 1103–1117, Apr. 2010.
- [20] S. Haykin, "Cognitive radar: A way of the future," *IEEE Trans. Signal Process. Mag.*, vol. 23, no. 1, pp. 30–40, Jan. 2006.
- [21] J. R. Guerci, *Cognitive Radar: The Knowledge-Aided Fully Adaptive Approach*. Norwood, MA: Artech House, 2010.
- [22] N. A. Goodman, P. R. Venkata, and M. A. Neifeld, "Adaptive waveform design and sequential hypothesis testing for target recognition with active sensors," *IEEE Trans. Signal Process.*, vol. 1, no. 1, pp. 105–113, Jun. 2007.
- [23] S. Haykin, Y. Xue, and T. N. Davidson, "Optimal waveform design for cognitive radar," in *Proc. 42th Asilomar Conf. Signals, Syst. Comput.*, Pacific Grove, CA, Oct. 2008, pp. 3–7.
- [24] F. Gini, A. De Maio, and L. Patton, *Waveform Design and Diversity for Advanced Radar Systems* Inst. Eng. Technol. Series 22, 2012.
- [25] M. Hurtado, T. Zhao, and A. Nehorai, "Adaptive polarized waveform design for target tracking based on sequential Bayesian inference," *IEEE Trans. Signal Process.*, vol. 56, no. 3, pp. 1120–1133, Mar. 2008.
- [26] S. P. Sira, Y. Li, A. Papandreou-Suppappola, D. Morrell, D. Cochran, and M. Rangaswamy, "Waveform-agile sensing for tracking," *IEEE Signal Process. Mag.*, vol. 26, no. 1, pp. 53–64, Jan. 2009.
- [27] S. Sen and A. Nehorai, "OFDM MIMO radar with mutual-information waveform design for low-grazing angle tracking," *IEEE Trans. Signal Process.*, vol. 58, no. 6, pp. 3152–3162, Jun. 2010.
- [28] D. J. Kershaw and R. J. Evans, "Optimal waveform selection for tracking systems," *IEEE Trans. Inf. Theory*, vol. 40, no. 5, pp. 1536–1550, Sep. 1994.
- [29] D. J. Kershaw and R. J. Evans, "Waveform selective probabilistic data association," *IEEE Trans. Aerosp. Electron. Syst.*, vol. 33, no. 4, pp. 1180–1188, Oct. 1997.
- [30] J. Yuanwei, J. Moura, and N. O'Donoghue, "Time reversal in multiple-input multiple-output Radar," *IEEE Trans. Signal Process.*, vol. 4, no. 1, pp. 210–225, Feb. 2010.
- [31] S. P. Sira, A. Papandreou-Suppappola, D. Morrell, and D. Cochran, "Waveform-agile sensing for tracking multiple targets in clutter," in *Proc. Conf. Inf. Sci. Syst. Special Session on Waveform Adaptive Sensing*, Princeton, NJ, Mar. 2006, pp. 1418–1423.
- [32] S. Suvorova, D. Musicki, B. Moran, S. Howard, and B. La Scala, "Multi step ahead beam and waveform scheduling for tracking of maneuvering targets in clutter," in *Proc. IEEE Int. Conf. Acoust., Speech, Signal Process.*, Philadelphia, PA, Mar. 2005, pp. 889–892.
- [33] H. L. Van Trees, *Detection, Estimation, and Modulation Theory*, 3rd ed. Hoboken, NJ: Wiley, 1968.
- [34] I. Reuven and H. Messer, "A Barankin-type lower bound on the estimation error of a hybrid parameter vector," *IEEE Trans. Inf. Theory*, vol. 43, no. 3, pp. 1084–1093, May 1997.
- [35] L. Zuo, R. Niu, and P. Varshney, "Conditional posterior Cramér-Rao lower bounds for nonlinear sequential Bayesian estimation," *IEEE Trans. Signal Process.*, vol. 59, no. 1, pp. 1–14, Jan. 2011.
- [36] P. Stoica and R. L. Moses, *Spectral Analysis of Signals*. Upper Saddle River, NJ: Prentice-Hall, 2005.
- [37] W. Huleihel, J. Tabrikian, and R. Shavit, "Optimal sequential waveform design for cognitive radar," in *Proc. ICASSP*, Mar. 2012, vol. 2, pp. 2457–2460.
- [38] S. Boyd and L. Vandenberghe, *Convex Optimization*. New York: Cambridge Univ. Press, 2004.
- [39] S. P. Wu, L. Vandenberghe, and S. Boyd, "Determinant maximization with linear matrix inequality constraints," *SIAM J. Matrix Anal. Appl.*, vol. 19, no. 2, pp. 499–533, Apr. 1998.
- [40] S. P. Wu, L. Vandenberghe, and S. Boyd, *Software for Determinant Maximization Problems. Users Guide, Alpha Version*. Stanford, CA: Stanford Univ. Press, 1996.
- [41] H. Li, *Complex-Valued Adaptive Signal Processing Using Wirtinger Calculus and Its Application to Independent Component Analysis*. Baltimore, MD: Univ. Maryland Baltimore County, 2008.
- [42] S. Chib and E. Greenberg, "Understanding the Metropolis-Hastings algorithm," *Amer. Statist.*, vol. 49, no. 4, pp. 327–335, Nov. 1995.
- [43] A. J. Weiss and E. Weinstein, "A lower bound on the mean square error in random parameter estimation," *IEEE Trans. Inf. Theory*, vol. 31, no. 5, pp. 680–682, Sep. 1985.
- [44] J. Tabrikian and J. L. Krolik, "Barankin bounds for source localization in an uncertain ocean environment," *IEEE Trans. Signal Process.*, vol. 47, no. 11, pp. 2917–2927, Nov. 1999.
- [45] D. S. Bernstein, *Matrix Mathematics: Theory, Facts, and Formulas*, 2nd ed. Princeton, NJ: Princeton Univ., 2009.



Wasim Huleihel received the B.Sc. and M.Sc. degrees in electrical engineering from the Ben-Gurion University of the Negev, Beer-Sheva, Israel, in 2012 and 2013, respectively.

Currently, he is working toward the Ph.D. degree in electrical engineering at the Technion Institute of Technology, Haifa, Israel. His research interests are in the areas of statistical signal processing and information theory.



Joseph Tabrikian (S'89–M'97–SM'98) received the B.Sc., M.Sc., and Ph.D. degrees in Electrical Engineering from the Tel-Aviv University, Tel-Aviv, Israel, in 1986, 1992, and 1997, respectively.

During 1996–1998, he was with the Department of Electrical and Computer Engineering, Duke University, Durham, NC, as an Assistant Research Professor. He is now with the Department of Electrical and Computer Engineering, and Ben-Gurion University of the Negev, Beer-Sheva, Israel. His research interests include estimation and detection

theory and array signal processing.

Dr. Tabrikian has served as an Associate Editor of the IEEE TRANSACTIONS ON SIGNAL PROCESSING during 2001–2004, and since 2011, and as an Associate Editor of the IEEE SIGNAL PROCESSING LETTERS since 2012. He has been a member of the IEEE SAM Technical Committee since 2010 and was the Technical Program Co-Chair of the IEEE SAM 2010 workshop. He is a coauthor of four award-winning papers in different IEEE conferences.



Reuven Shavit (M'82–SM'90) was born in Romania on November 14, 1949. He received the B.Sc. and M.Sc. degrees in electrical engineering from the Technion-Israel Institute of Technology, Haifa, in 1971 and 1977, respectively, and the Ph.D. degree in electrical engineering from the University of California, Los Angeles, in 1982.

From 1971 to 1993 he worked as a Staff Engineer and Antenna Group Leader in the Electronic Research Laboratories of the Israeli Ministry of Defense, Tel Aviv, where he was involved in the design of reflector, microstrip, and slot antenna arrays. He was also a part-time lecturer at Tel Aviv University, teaching various antenna and electromagnetic courses. From 1988 to 1990, he was associated with ESSCO, Concord, MA, as a Principal Engineer involved in scattering analysis and tuning techniques of high-performance ground-based radomes. Currently, he is with Ben-Gurion University of the Negev, as a Professor doing research on microwave components and antennas. His present research interest is in the areas of smart antennas, tuning techniques for radomes and numerical methods for design microstrip, slot and reflector antennas.